INSTITUTO SUPERIOR DE ENGENHARIA DE LISBOA

Área Departamental de Engenharia Civil

Determination of stresses around a cylindrical single pile caused by horizontal movements of soft soils with the finite element method

Marco André da Silva Gomes

Mestrado em Engenharia Civil

Dissertação para obtenção do grau de Mestre em Engenharia Civil

na Área de Especialização em Estruturas

Orientadores

Prof. Dr.-Ing. habil. Christian Moormann, Presidente do IGS Stuttgart

Dipl.-Ing. Johannes Aschrafi, PhD Student IGS Stuttgart

Mestre, António Lopes Cabral, Professor Adjunto do ISEL

Júri:

Mestre, Cristina Ferreira Xavier de Brito Machado, Prof. Coordenadora do ISEL

Doutor, António Gabriel Ferreira de Sousa Coutinho, Investigador Principal do LNEC

Fevereiro de 2013

ACKNOWLEDGMENTS

It has been a great pleasure for me to have the opportunity to develop my Master Thesis in the Institute für Geotechnik from Universität Stuttgart (IGS). I would like to express my deepest sense of gratitude to my advisor, the president of IGS Prof. Dr.-Ing. habil. Christian Moormann, to Dipl.-Ing. Johannes Aschrafi, and to all the members of IGS for their patient guidance, support, encouragement, and excellent advice throughout my research project.

My thanks also to my advisor in Portugal, Eng. António Cabral, who had an important role in this project from the beginning, and to Dr. Sérgio Martins Oliveira and Eng. João Alfredo Santos, that were always available to help.

I take this opportunity to express my profound gratitude to my classmates, José Vieira and André Teixeira, for their companionship and friendship over these 5 years.

My final, and heartfelt, acknowledgment must go to my parents, to my sister, to my nephew and to Sabrina Pröll, for their support and advices.

ABSTRACT

This study was carried out with the aim of modeling in 2D, in plain strain, the movement of a soft cohesive soil around a pile, in order to enable the determination of stresses resulting along the pile, per unit length. The problem in study fits into the large deformations problem and can be due to landslide, be close of depth excavations, to be near of zones where big loads are applied in the soil, etc. In this study is used an constitutive Elasto-Plastic model with the failure criterion of Mohr-Coulomb to model the soil behavior. The analysis is developed considering the soil in undrained conditions. To the modeling is used the finite element program PLAXIS, which use the Updated Lagrangian - Finite Element Method (UL-FEM). In this work, special attention is given to the soil-pile interaction, where is presented with some detail the formulation of the interface elements and some studies for a better understand of his behavior. It is developed a 2-D model that simulates the effect of depth allowing the study of his influence in the stress distribution around the pile. The results obtained give an important base about how behaves the movement of the soil around a pile, about how work the finite element program PLAXIS and how is the stress distribution around the pile. The analysis demonstrate that the soil-structure interaction modeled with the UL-FEM and interface elements is more appropriate to small deformations problems.

Key Words: Rigid Piles; Passive Piles; Soil Movements; Lateral Loading; Soil-Pile Interaction; Large Deformations; Interface Finite Elements.

RESUMO

Este trabalho final de mestrado tem como objectivo efectuar a modelação bidimensional (2D), do movimento de um solo argiloso à volta de uma estaca de forma a possibilitar a determinação das tensões resultantes ao longo da estaca por unidade de comprimento. O problema em estudo enquadra-se no problema de grandes deformações e pode dever-se: a um deslizamento de terras; a encontrar-se junto a escavações profundas; a encontrar-se junto a uma zona onde grandes cargas sejam transmitidas ao solo; etc. Neste estudo é utilizado um modelo constitutivo elásto-plástico com o critério de rotura de Mohr-Coulomb para modelar o comportamento do solo. A análise é efectuada considerando o solo em condições não drenadas. Será utilizado o programa de elementos finitos PLAXIS que usa o Update Lagrangian - Finite Element Method (UL-FEM). Neste trabalho é dada uma especial atenção à interação solo-estaca, onde é apresentado com algum pormenor a formulação dos elementos de interface e alguns estudos paramétricos que permitem um melhor entendimento do seu comportamento. É desenvolvido um modelo bidimensional que simula o efeito da profundidade, permitindo assim o estudo da sua influência na distribuição das tensões à volta da estaca. Os resultados obtidos neste trabalho fornecem uma importante base acerca de como funciona o movimento do solo à volta de uma estaca, o programa de elementos finitos PLAXIS e a distribuição das tensões na estaca. A análise efectuada mostra que a modelação da interação solo-estaca com o UL-FEM e com os elementos de interface é mais adequada para problemas de pequenas deformações.

Palavras Chave: Estacas Rígidas; Estacas Passivas; Movimento do Solo; Interação Solo-Estaca; Grandes Deformações; Elementos Finitos de Interface.

CONTENTS

LIST OF FIGURES

LIST OF TABLES

LIST OF SYMBOLS

Δu - displacement discontinuity

Δu^e - elastic displacement discontinuity

Δu^p - plastic displacement discontinuity

δu - virtual displacements

δε - virtual strains

δ{Δu} - virtual displacement discontinuity

δ - displacement

σ - normal stress

τ - shear stress

ν - Poisson's ratio

φ - friction angle

ψ - dilatancy angle

ε - volumetric strain

c - cohesion

c_u - undrained cohesion

D - Pile diameter

D' - elasticity matrix

E - Young's modulus

E_u - Undrained Young's modulus

G_i - shear modulus

$E_{oed,i}$ - one-dimension compression modulus

K_s - elastic shear interface stiffness

K_n - elastic normal interface stiffness

S_u - undrained shear strength

u - uniform displacement applied in the left and right boundary of the model in study

u_n - elastic gap displacement

u_t - elastic slip displacement

t_i - virtual thickness

t_c - traction transmitted by the interface

1 INTRODUTION

Pile foundations are used to support the heavy structure and can act in the dual role of carrying the applied load to deeper, strong layers, and also of reinforcing the soil. When piles are subjected to soil movements, these piles are known as passive piles. Soil movement is encountered in practice when piles are placed in an unstable slope, landslides, adjacent to deep excavation, tunnel operation, marginally stable riverbank with high fluctuating water level and also in piles supporting bridge abutment adjacent to approach embankments. On other hand, active piles referred to a pile subjected to a external vertical and/or horizontal force.

Design of piles under lateral load is commonly based on two criteria. The first criterion calculates the ultimate load and considers a general factor of safety or specify resistance reduction factors and load factors. The second criterion is based on an allowable lateral displacement. In this study, due to limitations of the model in 2-D, is not possible to study the lateral displacement of the pile getting restricted to the study of the ultimate load on the pile and in the generation of stresses around the pile.

1.1 Objective

The main objective of this research work is to develop a model in order to study the behavior of a single pile subject to a lateral loading. The research work will be concentrated in the determination of stresses around a cylindrical single pile and the ultimate force applied, caused by horizontal movements of cohesive soft soils.

1.2 Methodology

Initially, the main characteristics and limitations of the problem was identified, in order to define possible solutions, based on literature about similar problems, and target the research in the right way.

The literature review centered on analyze of lateral load on piles due to movement of soils. Special attention was given to movement of soft soils. Numerical models, geometry, soils characteristics and all the information needed to realize a numerical analyze was studied in this chapter.

As the next step, was explored the tools offered by PLAXIS in the 2-D version, with the finality of develop the best model for each element.

Taking into account the previous information, the modeling of the problem was developed in 2-D, making the study of the problem in all its variables, from the interface, the resistance and stiffness parameters of the soil. It was also assessed the influence of depth in the results, as well the "roughness" of the interaction pile-soil.

After the conclusion with the program PLAXIS, a research about new tools and methods was developed. The solution of ABAQUS was chosen and a new study about the tools offered by ABAQUS was developed. A new model was developed and a overview is presented.

1.3 Structure of the thesis

In this point the structure adopted for develop this thesis is presented. The thesis is divided in 6 chapters. Following the main chapters is presented and a brief introduction is presented:

Chapter 1 - Introduction to the thesis. Is given an introduction to the main problem in which is based the thesis and is presented the objective, the methodology and the structure of the thesis.

Chapter 2 - Literature review. Is presented the research work developed in order to take notice about what was been done on this area in the last years. The chapter is divided in theoretical methods, numerical methods, laboratory and field tests and distribution of soil pressure and displacements.

Chapter 3 - Finite element program - PLAXIS. Is presented the main functions from the program used in this research work. The functions described are: mesh generation; constitutive models; undrained conditions; update mesh calculation; and interface elements.

Chapter 4 - 2-D analysis of a single pile. This chapter describes the methodology used in all the processes of modeling, the main problems founded and how they were solved and presented the results obtained. The chapter is divided in idealized model in 2-D, mesh generation, interface, influence of depth, influence of roughness in the interface, soil displacements and parametric study.

Chapter 5 - Further study. In this chapter is presented a more detailed study about critical topics founded during the develop of the thesis. A deep explanation about the problem is presented and a solution is explored.

Chapter 6 - Conclusion. In this chapter is presented the conclusions of the research study developed. Is given an overview about what can be done in future studies in this area.

2 LITERATURE REVIEW

2.1 Introduction

After a literature research work about the subject in study, it is presented below the most important developments carried out and reported in literature, divided in four sections: a) theoretical methods; b) numerical methods; c) laboratory and field tests; and d) distribution of soil pressure and displacements.

The propose of this literature review is to establish a theoretical framework for the topic in study, define key terms, definitions and terminology, and to help to clarify the topic of this thesis.

2.2 Theoretical Methods

The theoretical methods are divided in pressure-based methods and in displacement-based methods. This point as a important influence in the definition and study of the boundary conditions used in the model.

2.2.1 Pressure-Based Methods

Ito and Matsui (1979) used plastic extrusion theory to postulate a method for determining the theoretical equation of lateral forces acting on piles in a row though soil mass above the sliding surface. They have presented an equation to obtained the lateral forces acting on a pile per unit depth of soil layer, which considers the distance between piles and assuming that the Mohr-Coulomb's plastic condition occurs in the surrounding ground just around the piles, as we can see in Ito and Matsui (1975, 1977 and 1978). In 1982, Matsui check the validity of the theoretical equation presented, using a series of model test for various conditions of the pile and the soil.

Viggiani (1981) used a limit equilibrium method to analyze the mechanism of interaction between a sliding soil mass and a pile crossing it and penetrating the

stable underlying soil. He has presented six different mechanisms were the failure may occur, which depends from the geometry of the problem, the yield moment of the pile section and the strength of the stable and sliding soil.

Garb and Borden (1990) used a Force-equilibrium model to derive a theoretical solution for the lateral capacity of rigid piles embedded in cohesionless and c-ø soil profile having a sloping ground surface. A slope model is used in the construction of the P-y curves used in the analysis of laterally loaded piles. The lateral soil resistance was derived by considering the pile as a translating cylinder moving into the soil.

Stewart (1999) used a upper bound plasticity method to estimate the undrained collapse load of laterally loaded piles in clay. For the case of level ground, the method yields results are very similar those from Broms (1964) approach. The effect of a slope adjacent to the pile was incorporated by truncating part of the assumed collapse mechanism. He has concluded that the reduction factor in any case depends largely on the distance of the pile from the crest of the slope, the slope gradient and the length to diameter ratio of the pile.

Loehr et al. (2004) developed a basic analysis methodology for predicting the resistance provided by individual slender reinforcing members for slope stabilization using pressure-based method. The method uses a limit state design approach where in a series of potential failure modes are considered to develop the distribution of limiting resistance forces along a reinforcing member.

Sheng (2011) presents a review of constitutive models for unsaturated soils. In particular, it focuses on the fundamental principles that govern the volume change, shear strength, yield stress, water retention and hydromechanical coupling. Alternative forms of these principles are critically examined in terms of their predictive capacity for experimental data, the consistency between these principles and the continuity between saturated and unsaturated states.

2.2.2 Displacement-Based Methods

Poulos (1973) presented a boundary element method for the analysis of a single pile in a soil subjected to lateral soil movement. This analysis is an extension of analyses previously developed for laterally loaded piles in which the soil is assumed to be an ideal elastic-plastic material. The method requires an input of the magnitude of the free-field soil movement at each depth and the ultimate soil pressure acting on piles.

Hull et al. (1991) investigated the behavior of a pile in an unstable slope using a displacement-based method. The pile response, when subjected to passive loads, is analyzed using a modified boundary element method developed by Poulos (1973). This method takes into consideration the relative displacements between the soil and the pile, the relative stiffness of the pile and soil, as well as the finite length of pile.

Lee et al. (1995) presents a simplified approach to the study of a row of piles used for slope stabilization. The approach is based in an uncoupled formulation in which the pile response and slope stability are considered separately. The pile response when subjected to external lateral soil movements from slope instability is analyzed by a modified boundary element method.

Jeong et al. (2003) presents a simplified numerical approach for analyzing the slope/pile system subjected to lateral soil movements. The approach is based in an uncoupled analysis were the pile response and slope stability are considered separately, and the Bishop's simplified method of slope stability analysis is extended to incorporate the soil-pile interaction and evaluate the safety factor of the reinforce slope. With this study was been found that the factor of safety in slope is much more conservative for an uncoupled analysis than for a coupled analysis based on three-dimensional finite element analysis.

Zhang (2009) develop a method for nonlinear analysis of laterally loaded piles in cohesionless soil. The method assumes that both the ultimate soil resistance and the modulus of horizontal subgrade reaction increases linearly with depth.

To determine the ultimate soil resistance and the modulus of horizontal subgrade reaction, related expressions are selected by reviewing and assessing the existing methods. In 2012, Zhang propose a nonlinear mechanical model for piles subjected to lateral soil movement, based on the Winkler elastic model. In this model the plastic deformation of surrounding soils was taken into account using a simplified elastic-plastic constitutive model.

Huang et al. (2011) developed a simplified method to estimate the vertical movement and load distribution on pile raft foundations subjected to ground movements induced by tunneling based on a two-stage method. In this method, the Loganathan-Poulos (1998) analytical solution is used to estimate the free soil movement induced by tunneling in the first stage. In the second stage, composing the soil movement to the pile, the governing equilibrium equations of piles are solved by the finite difference method.

Several investigators also study this subject, presenting methods to calculate the stresses and displacements, between them we can mention Katzenbach et al. (2007), Zhang et al. (2011), Zhang et al. (2012).

2.3 Numerical Methods

The numerical methods are divided in finite element methods, subgrade reaction methods and boundary element methods.

2.3.1 Finite Element Methods

The Finite Element Method (EFM) currently presents one level of development which allows its use by most designers of structures. It is verified today that due to the complexity of software development, most of the users are limited to their use and interpretation of data. Faced with this problem, it is indispensable that engineering students have a thorough knowledge of the EFM.

Rowe and Poulos (1979) propose a finite element technique for the analysis of the undrained behavior of soil slopes reinforced by piles groups. An elastic-plastic model was employed to model the soil, and the soil was allowed to flow past the piles once the limiting pressure was reached. The stiffness of the plane strain piles was determined from an approximate correlation of the lateral response of pile groups between predictions from a 3-D elastic analysis and a 2-D finite element analysis. Randolph (1981) used a similar technique where the piles were replaced by an equivalent sheet-pile wall with flexibility equal to the average of the piles and soil it replaced. This analysis can accommodate pile groups and has been used to analyze pile groups near embankments.

Finno et al (1991) employed a plane-strain finite element program to study the behavior of sheet-pile wall adjacent to a nearby deep excavation. The program is a simulation of the excavation process and determines the soil movement and pile-cap movement. The bending moments in the pile are calculate using the pile deformations. With the bending moments the effects of the movements on their integrity are evaluate.

As reported by Poulos and Davis (1980), the first attempts to study the lateral behavior of piles included two-dimensional finite element models in the horizontal plane. Several investigations have attempted to study the behavior of pile under lateral load using 3D finite element analysis, among then we can mention Yang et al. (2005), Miao et al. (2005), Karthigeyan et al. (2007), Kahyaoglu et al. (2009), Liyanapathirana et al. (2010), and Liang et al. (2002 and 2010).

Bransby (1996) carried out a two-dimensional finite element analyses to study undrained soil deformation around piles displaced laterally through soil. The study show the diference between load-transfer relationships for laterally loaded pile groups, being that the load-transfer p-δ cuves are applicable for design during passive lateral loading, and the load transfer p-y curves are applicable for active lateral loading.

2.3.2 Others Methods

In this point will be presented the numerical methods considered as relevant.

2.3.2.1 Subgrade reaction method

Terzaghi (1955) presents a propose for the factors which determine the value of the coefficients of both vertical and horizontal subgrade reaction of cohesionless sand and stiff clay, and propose numerical values for the constants which appear in the equations defining these coefficients. It contains also brief reviews of the practical application of the theories of subgrade reaction.

Kobayashi et al. (2007) carried out a estimation of horizontal subgrade reaction coefficient by inverse analysis. The subgrade reaction coefficient of a foundation soil in an open pier has been identified using an extended Kalman filter based on measurements taken during in situ horizontal loading tests on a pile.

Kim et al. (2010) investigate the load distribution and deflection of large diameter piles by lateral load transfer method (p - y curve). A framework for determining a p-y curve is calculated based on the surrounding soil stress and it was carried out the appropriate parametric studies needed for verifying the p-y characteristics.

Cai et al. (2011) reports a subgrade reaction solution for piles used to stabilize landslides where the sliding layer laterally moves with a displacement decreasing linearly with depth. The developed subgrade reaction solution can deal with the case in which pile segments in both sliding and stable layers are not flexible, and can also calculate the pile response under the additional resistance required to stabilize the landslide.

2.3.2.2 Boundary element method

Alarcon et al. (1989) present a boundary element approach for time harmonic axisymmetric problems using the complete space point load fundamental solution. The approach is applied to the computation of the dynamic stiffness functions of rigid circular foundations on layered viscoelastic soils.

Mendonça et al. (2000) presents a boundary element method formulation for the static analysis of piled rafts in wich all the interactions between the plates, the pile and the soil are simultaneously considered.

Almeida et al. (2006) propose to use the boundary element method to analyze soil-foundations interactions. Each region occupied by a soil layer or by a foundation component is handled as a 3D isotropic, elastic and homogeneous domain, and is analyzed by boundary element method.

Various authors have developed models that use the Boundary element method and the finite element method together, using the Finite element method for modeled the pile and the boundary elements method for modeled the soil. As example we have Matos Filho et al. (2005) Pedrón et al. (2007, 2011) and Millán et al. (2009).

2.4 Laboratory and Field Tests

This point is divided in laboratory and field tests. Is presented the main laboratory and field tests carried out about the subject in study.

2.4.1 Laboratory Tests

Adachi et al. (1989) conducted a series of two-dimensional laboratory model tests to study the mechanism of piles when subjected to lateral soil movements. They suggested that the extend of the arching effect for circular piles was different from that of rectangular piles, and the load acting on the circular piles was generally smaller than that acting on the rectangular piles by about 15%.

The test results showed that the load acting on piles increased with increasing spacing, and when the center-to-center spacing between piles was greater than 8 times the pile diameter, the piles behaved like a single pile.

Stewart et al. (1992) carry out a series of model tests on piles adjacent to embankment constructions using a geotechnical centrifuge. The safety factor against failure of the embankment was found to greatly influence the pile response, with significantly large bending moments and deflections developed for a safety factor of less than 1.7. The centrifuge tests give a direct insight into the behavior of piles subjected to subsoil movement and the results are considered to be of significant practical value.

Leung et al. (2000) carried out a centrifuge model test on untrusted deep excavation in dense sand and its influence on an adjacent single pile foundation behind the retaining wall. It is found that, in the case of stable wall, the induced pile bending moment and deflection decrease exponentially with increasing distance between the pile and the wall.

Ong et al. (2009) conducted a series of centrifuge model tests to investigate the behavior of pile groups of various sizes and configurations behind a retaining wall in very soft clay. With a simulate of a initial stage of an excavation prior to strutting, the test results reveal that the induced bending moment on an individual pile in a free-head pile group is always smaller than on a corresponding single pile located at the same distance behind the wall.

Chandrasekaran et al. (2010) carried out a static lateral load test on 1x2, 2x2, 1x4, and 3x3 model pile groups embedded in soft clay. The effects of pile spacing, number of piles, embedment length, and configuration on pile-group interaction were investigated. It has been found that the lateral capacity of piles in 3x3 groups at three diameter spacing is about 40% less than of the single pile. Group interaction causes 20% increase in the maximum bending moment in piles of the groups with three diameter spacing in comparison to the single pile.

2.4.2 Field Tests

Kalteziotis et al. (1993) described a case where more than 30 piles, arranged in two rows, were employed with success to stabilize a moving slope. The results revealed that the soil displacement profile was triangular with depth, with the maximum at the top of the soil, and there existed an arching effect which tended to stop soils from squeezing through piles.

Castelli et al. (1999) presents a in situ tests concerning the behavior of laterally loaded single piles in cohesive soils. Have been compiled a computer code for the analysis of the behavior of the simple pile subjected to horizontal loads based on a pile finite element discretization and validated by in situ full scale tests (Castelli et al. (1995)). The model takes into account the non-linearity of the soil-pile interaction employing hyperbolic or cubic parabolic p-y curves.

A few authors have used the test fields and numerical analysis to determine the load distribution and deformation of piles in different conditions; between them we can mention the following: Janoyan et al. (2001); Lin et al. (2005); Karthigeyan et al. (2007); Kim et al. (2009); and Ching et al. (2010). Some conclusions were drawn: the deformed shape of the pile is affected by the stiffness of the pile; and the soil pressure acting on the pile may increase or decrease with decreasing pile spacing.

2.5 Distribution of Soil Pressure and Displacements

Knowledge of the distribution of soil pressure and soil displacement along the depth is very important for reasonable predictions by both pressure-based methods and displacement-based methods. So is important have information acquired from the practice to have a better theoretical predictions. Based on the above, is presented below some experiences acquired.

2.5.1 Soil Pressure Distribution

Ito & Matsui (1975) reported measurements of lateral soil force acting on a row of piles. It was measured the forces acting on the piles from electrical strain gauges.

Escario & Uriel (1989) showed a measure profile of lateral soil pressure acting on a pier supporting a viaduct due a near embankment construction.

Randolph &Springman (1991) proposed that the distribution of the soil pressure against piles should be parabolic, with the maximum value at the center of the layer.

2.5.2 Soil Displacement Distribution

Heyamn&Boersma (1961) showed a measure profile of lateral soil displacement caused by an adjacent embankment built 5 m away from the piles, and the soil displacements were measured after each extension of the embankment.

Suzuki (1988) studied reported cases from 11 sites in relation to embankment constructions and presented some profiles of horizontal soil displacement at the toe of each embankment.

Kalteziotis et al. (1993) showed a measure profile of lateral soil displacement caused by a moving slope. The measure shows that the soil behavior is different depending on the direction.

3 FINITE ELEMENTS ANALYSIS PROGRAM - PLAXIS

For the development of this work the numeric tool used in the stress-deformation analyses was the finite element program PLAXIS 2D version 2011. In this chapter are presented the main tools offered by PLAXIS and used in this research work.

3.1 Introduction to the program

The development of PLAXIS began at Delft University of Technology as an initiative of the Dutch Ministry of Public Works and Water Management. The program was develop with the propose to carried out a 2D finite element code for the analysis of river embankments in soft soils, but quickly spread to all geotechnical areas. Only in 2001 the 3D finite element calculations were developed, resulting in the 3D Tunnel program. With this programs it is possible to generate automatically the mesh in both 2D and 3D, the simulation of interface and beam elements, and has a graphic interface of in and out of results.

Following will be presented the main characteristics of PLAXIS program, the constitutive models and the analyze type possible.

3.2 PLAXIS program

PLAXIS is a finite element package intended for the two-dimensional or three-dimensional analysis of deformation, stability and groundwater flow in geotechnical engineering. It is part of the PLAXIS product range, a suite of finite element programs that is used worldwide for geotechnical engineering and design.

The program work in windows environment and is constituted by the following modules or sub-programs:

PLAXIS "input": Module for entrance of geometry, dispositions of the elements, boundary conditions, properties of the materials, loads and initial conditions of stresses or deformation from the problem, the soil behavior model and the boundary conditions. In this module is also generated the finite element mesh.

PLAXIS "Calculations": Carried out the calculation from the stress and deformation state resultant of the loading of the problem. The calculation finish when is reached the number of steps of loads and iterations determinates on one level of admissive load level. In these modules are defined also the different stages of loading, by applications of external loads, by excavation or by construction. This sub-program only takes into account deformation analysis and makes a distinction between one plastic calculation, one density analysis and one analysis with update mesh generation (normally used for big deformations).

PLAXIS "Output": The module of output of the results is very friendly allowing to view the deformations, the displacements and total or effective stresses. It is possible to obtain tables with the results of the displacements, deformations and total and effective stresses. Also generates graphics of forces, stresses, displacements and deformations in the deferent elements. It is possible to view the points where the material have plasticized or have been subject to tensile stresses.

Between the main features of the program it can be referred: the static drained and undrained analysis; the analysis using Biot theory for coupled consolidation; the choose of different constitutive relations; the diversity of loading conditions due to external forces, displacements, nodal pressures or flow imposed; the algorithm for the automatic calculation in the determination of the increase in load and time, in case of non linear analysis and; the possibility to realize analysis in different phases.

3.2.1 Mesh generation

The program PLAXIS allow one procedure of automatic generation of the mesh, were the geometry is divided in triangular elements, in the form of basic elements and compatible structural elements. The program has triangular elements with 6 and 15 nodes in the 2D version. For the elements with 6 nodes, the stiffness matrix is evaluated for numeric integration, using one total of three gauss points (tension points). The element with 15 nodes are compounds by twelve gauss points and is more powerful than the 6 nodes elements. Although the use of 15 nodes leads to a memory consumes relatively high what leaves to a high computational time, this type of elements were chosen for the calculations due to the specificity of the problem.

The mesh generation takes into account the position from the points and lines in the geometric model such as the exact layers position, loads and structures are taking into account in the finite element mesh. The generation process of the mesh is based on the robust triangle principle, which looks for optimized triangles, resulting in a non-structured mesh. The behavior of that type of mesh is better than the structured mesh. Additionally, for the generation of the mesh, is made a transformation of the data entrance (properties, boundary conditions, materials parameters, etc.) from the geometric model (points, lines and regions) for the finite element mesh (elements, nodes and stresses points).

The precision of the results depends of the form and dimensions of the mesh used for represent the physic system. Finest meshes tend to better results. With this in mind, the program PLAXIS allow a finest mesh in the more sensible points.

3.2.2 Constitutive models

The choose of the model that will be used in the simulations of the material behavior has a big importance for the results obtained been realistic. Soil and Rock tend to behave in a highly nonlinear way while under load. This nonlinear

deformation behavior can be modeled under various levels of solicitation. For the case in study two constitutive models will be used: Elastic-linear model and Mohr-Coulomb model. Following a brief description of this models are presented. Despite the Elastic-linear model does not represent the nonlinear behavior of the material, is a good model for introduction to the Mohr-Coulomb model.

3.2.2.1 Elastic-linear model

This model represents Hooke's law of isotropic linear elasticity. The linear elastic model is too limited for the simulation of soil behavior. It is primarily used for stiff structures in the soil. It involves two basic elastic parameters, i.e. Young's modulus E and Poisson's ratio ν.

3.2.2.2 Mohr-Coulomb model

The linear elastic perfectly plastic Mohr-Coulomb model involves five input parameters, i.e. Young's modulus E and Poisson's ratio ν for the soil elasticity; friction angle φ and cohesion c for soil plasticity and ψ as a dilation angle. This Mohr-Coulomb model represents the transition between the elastic linear model and the most advanced models. It is recommended to use this model as the first realistic analysis of the problem considered.

Fig. 3.1 shows how works the linear elastic perfectly plastic of Mohr-Coulomb. While the Coulomb criterion (point 3.2.2.2) is not applied, the material has a linear elastic behavior. After the Coulomb criterion be applied the behavior is no more linear elastic and becomes perfectly plastic.

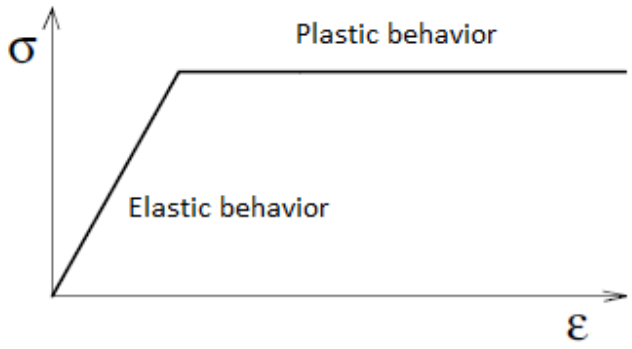

Fig. 3.1 - Representation of the linear elastic perfectly plastic model

3.2.3 Undrained conditions

The undrained analysis is appropriate when the permeability is low or rate of loading is high and when short behavior has to be considered. Implications of undrained soil behavior are:

- excess pore pressures are generated;
- no volume change. In fact, in PLAXIS small volumetric strains develop because a finite (but high) bulk modulus of water is introduced in the finite element formulation;
- and predicted undrained shear strength depends on soil model used.

The program PLAXIS allows different model schemes for modeling the undrained soil behavior, undrained A, B and C. The difference between this model schemes is explained below.

The undrained effective stress analysis can be carried out with effective stiffness and strength parameters (drainage type: Undrained A, Fig. 3.2.a), with effective stiffness parameters and undrained strength parameters (drainage type: Undrained B, Fig. 3.2.b), or with undrained strength and stiffness parameters (drainage type Undrained C, Fig. 3.2.c).

Fig. 3.2 shows the stress path and strength for the different undrained types available in PLAXIS. In the drainage type Undrained A the analysis is developed in terms of effective stresses and the undrained shear strength (S_u)

is a consequence of the model. The disadvantage of this model approach is that the undrained cohesion overestimates the undrained shear strength. In the drainage type: Undrained B the analysis is developed in terms of effective stresses and the stiffness parameters are calculated by the following expression:

$$E_u = \frac{3}{2}\frac{E}{1-\nu} \quad ; \quad \nu_u = 0{,}495 \qquad \text{Eq.1}$$

and the prediction of pore pressure are generally unrealistic. In the Drainage type Undrained C, the stiffness is modeled using an undrained Young's modulus E_u and an undrained Poisson ratio ν_u, and strength is modeled using an undrained shear strength S_u, with undrained cohesion (c_u) equal to undrained shear strength ($c_u = S_u$). The disadvantage of this approach is that no distinction is made between effective stresses and pore pressures, what means that only total stresses are obtained,

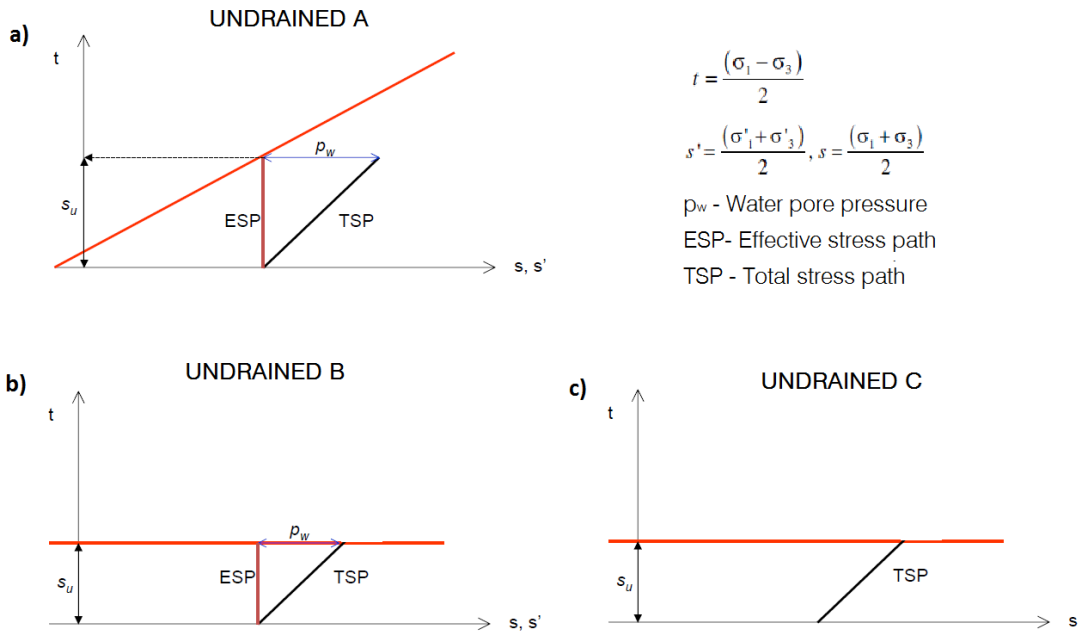

Fig. 3.2 - Stress path and strength according to: a) Undrained A; b) Undrained B; and c) Undrained C

3.2.4 Update mesh calculation

This option was developed to deal with situations of large deformations as problems where soils are soft and large deformations occur.

When large deformation theory is included in a finite element program some special features need to be considered:

- Is necessary to include additional terms in the structure stiffness to model the effects of large structural distortions on the finite element equations;
- It is necessary to include a procedure to model correctly the shear stress changes that occurs when finite material rotations occur. For this particular feature of large displacement theory is used in PLAXIS the co-rotational rate of Kirchhoff stress;
- It is necessary to update the finite element mesh as the calculation proceeds.

These calculation procedures are based on an approach known as "Updated Lagrangian formulation" (Bathe, 1982). The implementation of this formulation in PLAXIS is based on the use of advanced techniques which can be found in van Langen, 1991.

3.2.5 Interface elements

To model the interaction between two materials, the program PLAXIS has a element called "interface".

To define the properties of an interface exist two possibilities. The first is to assign a material to the interface, staying the interface defined with the properties of this material. The second is to use the parameter R_{inter}. This parameter has a reduction effect that is used to define the parameters from the interface, using reducing parameters from the material assigned for the surrounding soil. In general, for real soil-structure interaction the interface is weaker and more flexible than the surrounding soil, which means that the value

of R_{inter} should be less than 1. In Tab. 1 are presented some values proposed in Dennis Waterman (2006) for the value of R_{inter}.

Interaction	R_{inter}
Sand / Steel	0.6 - 0.7
Clay / Steel	0.5
Sand / Concrete	0.8 - 1.0
Clay / Concrete	0.7 - 1.0
Soil / Geogrid	1.0
Soil / Geotextile	0.5 - 0.9

Tab. 1 - Values for R_{inter} proposed in Dennis Waterman (2006)

3.2.5.1 Virtual thickness ti

For each interface is assigned one virtual thickness (Fig. 3.3), that is one virtual dimension used to obtain the properties of the interface material. The virtual thickness is defined as the virtual thickness factor multiplied by the medium size of the element. The medium size of the element is calculated by the mesh generation, in one gross global montage. The virtual thickness factor is defined by the user and varies between 0 and 1.

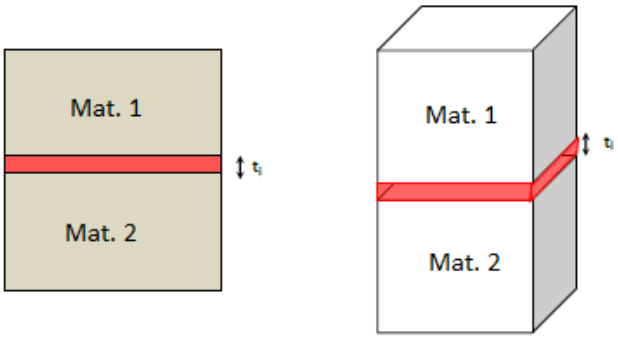

Fig. 3.3 - Representation of the virtual thickness in 2-D and 3-D

The virtual thickness is one of the key points for a correct modeling with interfaces elements. The influence of this factor in the interface displacements is shown in Eq.10 and Eq.11 at point 3.2.5.3. To explain the influence of this factor on the interface shear stress first is need to explain how the shear stress in a normal finite element is calculated. Fig. 3.4 shows a simple example of a deformed element where β is the angle of deformation. If β is zero no shear stress will be generated and if β increases also the shear stress will increase.

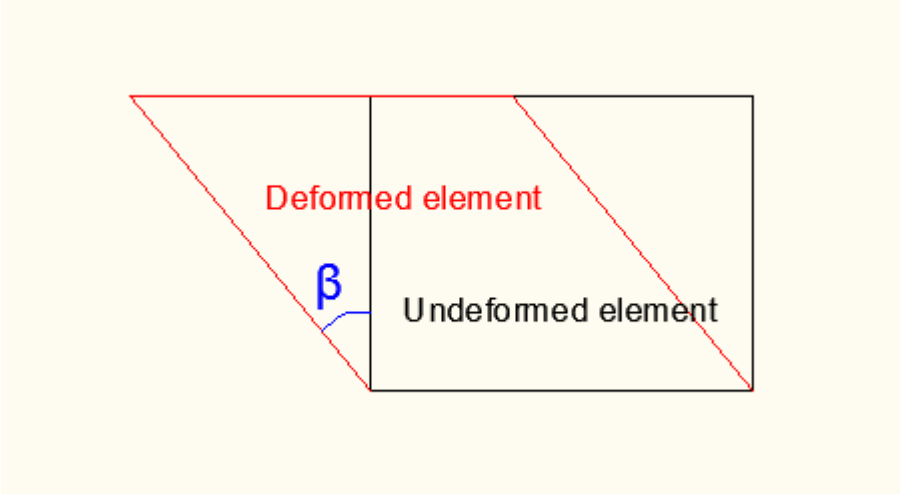

Fig. 3.4 - Finite element deformation

For the generation of the shear stress in the interface the principle is the same. Fig. 3.5 show a scheme of the deformation of the element and the interface thickness together. The shear stress in the interface is generated taking into account the deformation of the element which belongs and is limited taking into account the angle of deformation with the interface thickness. Therefore, with the increase of the interface thickness the deformation angle decrease and also the shear stress ($\beta<\alpha$). The influence of this parameter is better studied at point 4.8.5.

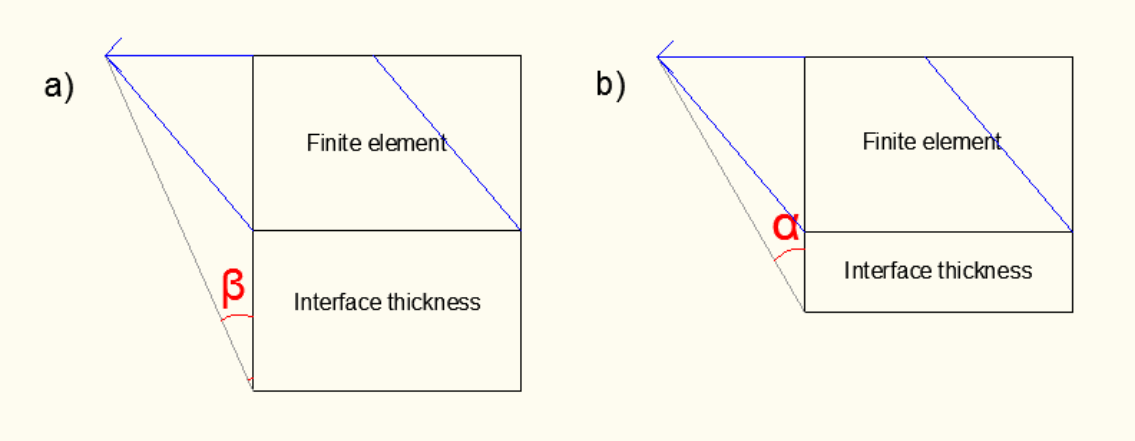

Fig. 3.5 - Interface element deformation for: a) bigger interface thickness; and b) small interface thickness

3.2.5.2 Interface using the Mohr-Coulomb model

The interface formulation used by PLAXIS is based on the formulation given by Koiter (1960), where the interface is seen as a displacement discontinuity in a continuum. Koiter (1960) gives the virtual work equation for a continuum with such a discontinuity:

$$\int_V \sigma^T \delta\varepsilon \, dV + \int_{S_c} t_c^T \delta \{\Delta u\} \, dS_c = \int_V \gamma^T \delta u \, dV + \int_{S_e} t_e^T \, \delta u \, dS_e \qquad \text{Eq.2}$$

where σ is the Cauchy stress tensor, δu and $\delta\varepsilon$ are the virtual displacements and strains, t_c is the traction transmitted by the interface, γ and te are body forces and surface tractions and $\delta\{\Delta u\}$ is the virtual displacement discontinuity.

Following the interface concept, slipping will occur when the interface traction t_c reaches some threshold value (Eq.3). Below this value no relative movement occurs and, as a result, the interface term in Eq.2 will disappear.

For an elastic-plastic relationship, combining linear elasticity and perfect plasticity, is used the following equation:

$$t_c = D' \, \Delta u^e = D' \, (\Delta u - \Delta u^p) \qquad \text{Eq.3}$$

Where the Coulomb criterion is used to distinguish between elastic and plastic parts.

The stiffness matrix for the interface elements is obtained using the integration points of Newton-Cotes. The position of this integration points (or stress points) is coincident with the position of the pairs nodes. So, for elements with 15 nodes are used 12 stress points. The elasticity matrix is given by the following expression:

$$D' = \begin{bmatrix} K_s & 0 \\ 0 & K_n \end{bmatrix} \qquad \text{Eq.4}$$

Where K_s and K_n is given by:

$$K_s = \frac{G_i}{t_i} \qquad \text{Eq.5}$$

and

$$K_n = \frac{E_{oed,i}}{t_i} \qquad \text{Eq.6}$$

With the shear modulus G_i and the one-dimensional compression modulus $E_{oed,i}$, for the case using the R_{inter} parameter, defined by:

$$G_i = R_{inter}^2 G_{soil} \quad \text{Eq.7}$$

$$\text{with} \quad G_{soil} = \frac{E_{soil}}{2(1+\nu_{soil})} \quad \text{Eq.8}$$

$$E_{oed,i} = 2G_i \frac{1-\nu_i}{1-2\nu_i} \quad \text{with} \quad \nu_i = \begin{cases} 0.450 & in\ drained\ conditions \\ 0.495 & in\ undrained\ conditions \end{cases} \quad \text{Eq.9}$$

For calculation with fully plastic behavior, the value of the elasticity matrix D is not important. In this case, $\Delta u = \Delta u^p$ leading the traction transmitted by the interface t_c set to zero.

3.2.5.3 Interface stiffness

When the interface is elastic then is possible have gapping and overlapping (relative movement parallel to the interface and relative displacement perpendicular to the interface) at the same time. The magnitudes of this displacement are given by:

$$\text{Elastic gap displacement } u_n = \frac{\sigma}{K_n} = \frac{\sigma\, t_i}{E_{oed,i}} \quad \text{Eq.10}$$

$$\text{Elastic slip displacement } u_t = \frac{\tau}{K_s} = \frac{\tau\, t_i}{G_i} \quad \text{Eq.11}$$

where G_i is the shear modulus of the interface, $E_{oed,i}$ is the one-dimensional compression modulus of the interface, t_i is the virtual thickness of the interface, K_n is the elastic interface normal stiffness and K_s is the elastic interface shear stiffness.

The behavior of the interface elements is one of the most difficult points to understand in this study. The formulation is complex and the way how this formulation is presented is not very clear for everyone. Taking this into account is following explained the formulation for the elastic gap displacement u_n the most simplified possible.

For a better understanding of the problem, first will be explained the behavior of a single pile subjected to a vertical load.

If we consider the Young's modulus E, the height of the pile L and the section area A, we can define the normal stiffness of the pile as $K_n = E*A/L$.

Recording the basic formulation of the finite element, we have:

$$Ku = F \overset{\div A}{\Leftrightarrow} \frac{K}{A}u = \frac{F}{A} \Leftrightarrow \frac{K}{A}u = \sigma \Leftrightarrow K_{A=1}.u = \sigma \Leftrightarrow u = \frac{\sigma}{K_{A=1}} \qquad \text{Eq.12}$$

where u is the displacement suffered by the pile due to the force F applied in the pile, and K is the stiffness of the pile. Making the relation with the interface element, where E is the Young's modulus of the interface, the height L is t_i and is considered a unitary area A, we have:

$$K_n = \frac{EA}{t_i} \overset{A=1}{\Longleftrightarrow} K_n = \frac{E}{t_i} \qquad \text{Eq.13}$$

that is

$$u_n = \frac{\sigma}{K_N} \Leftrightarrow u_n = \frac{\sigma}{E/t_i} \qquad \text{Eq.14}$$

what is in agreement with the formulation propose by the PLAXIS in Eq.10.

It is possible to conclude that the normal stiffness of the pile K_n is defined by the virtual thickness t_i (is virtual thickness because in reality this thickness is zero) and by the Young's modulus E. Is clear with this formulation that the stiffness parameters and the virtual thickness influence the elastic displacement of the interface. With the increase of these parameters the elastic displacements will decrease.

3.2.5.4 Mohr-Coulomb criterion

For the interface elements is assumed an elastic-plastic behavior. To distinguish between elastic behavior, where both gap and slip displacements can occur, and plastic behavior where permanent slip can occur, is adopted the

Mohr-Coulomb criterion. In this criterion a simple Mohr-Coulomb yield function $f(t)$ with a non-associate plastic potential $g(t)$ is used:

$$f(t) = \tau + \sigma_n \tan\varphi_i - c_i \quad \text{Eq.15}$$

$$g(t) = \tau + \sigma_n \tan\Psi_i \quad \text{Eq.16}$$

Where σ_N is the effective normal stress, τ the shear stress, φ_i are the friction angle and c_i is the cohesion of the interface. The friction angle φ_i and the cohesion c_i govern the strength. The dilatation angle Ψ_i controls the plastic dilatation. To prevent an over prediction of the plastic dilatation, the non-associate flow rule is used with $\Psi_i < \varphi_i$.

The rate of plastic slip is derived from the plastic potential function g(t):

$$\Delta u^p = \alpha\, \lambda \left(\frac{dg}{dt}\right) = \alpha\, \lambda \begin{bmatrix} 1 \\ \tan\Psi_i \end{bmatrix} \quad \text{Eq.17}$$

Where α works as a switch-on/switch-off coefficient defined by:

$$\alpha = 0 \quad \text{if} \quad f < 0 \quad or \quad \begin{bmatrix} \frac{df}{d\tau} & \frac{df}{d\sigma_n} \end{bmatrix} D\, \Delta u < 0 \quad \text{Eq.18}$$

$$\alpha = 1 \quad \text{if} \quad f = 0 \quad \text{or} \quad \begin{bmatrix} \frac{df}{d\tau} & \frac{df}{d\sigma_n} \end{bmatrix} D\, \Delta u \geq 0 \quad \text{Eq.19}$$

Now the multiplier λ can be solved from the consistence condition $f = 0$. Eq.14, 15 and 16 can be used for limit increments of shear stress and relative displacements. Solving the consistence condition $f = 0$, for the interface remain elastic the following equation should be respected:

$$|\tau| < -\sigma_N \tan\varphi_i + c_i \quad \text{Eq.20}$$

And for a plastic behavior:

$$|\tau| = -\sigma_N \tan\varphi_i + c_i \quad \text{Eq.21}$$

This behavior is easily visualized thought the following figure (Fig. 3.6):

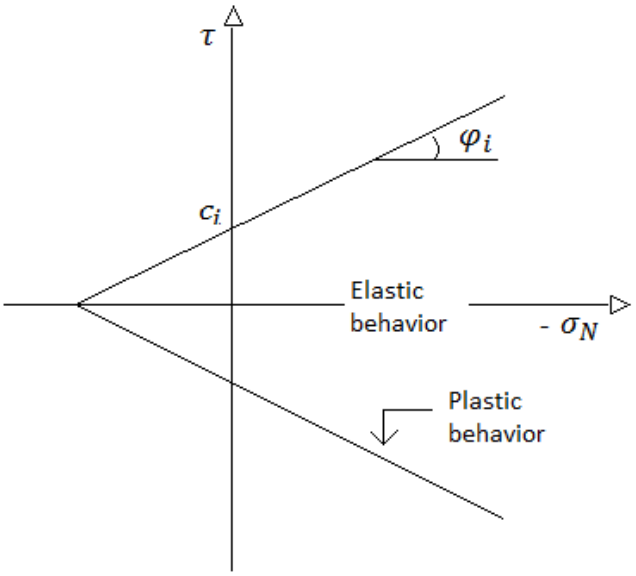

Fig. 3.6 - Mohr-Coulomb yield function

A Newton-Cotes scheme is used for the numerical integration of the stiffness matrix and related vectors. The position of the integration points coincides with the node pairs of the interface. This numerical integration leads to an lumped interface stiffness matrix, which suppresses possible stress oscillations.

In the case of use the R_{inter} the strength properties of interfaces are related to the strength properties of the surrounding soil. The value of R_{inter} cannot be more then 1, and works as a strength reduction factor. The interface properties are calculated by multiplying the strength reduction factor by the soil properties:

$$c_i = R_{inter}\, c_{soil} \qquad \text{Eq.22}$$

$$\tan \varphi_i = R_{inter}\ \tan \varphi_{soil} \qquad \text{Eq.23}$$

$$\psi_i = \begin{cases} 0° & for\ R_{inter} < 1 \\ \psi_{soil} & for\ R_{inter} = 1 \end{cases} \qquad \text{Eq.24}$$

When the option tension cut-off is used, the tension cut-off criterion is add to Coulomb's shear stress criterion following the rule:

$$\sigma_N < \sigma_{t,i} \quad \text{with} \quad \sigma_{t,i} = R_{inter}\, \sigma_{t,soil} \qquad \text{Eq.25}$$

3.2.5.5 Pile - Soil separation

When a pile is loaded laterally, tensile stresses will develop at the back of the pile. In case of frictional materials the soil behind the pile will collapse. This phenomenon can be simulated by using the tension cut-off criterion to the flow rule of the soil. However, this is not suitable to describe the behavior of laterally loaded piles in cohesive soils. In an undrained situation, the soil will be able to resist these tensile stresses up to the point where cavitations occur. However, for a small value of stress, the gap will occur and the pile can move almost freely through a previously formed slot. In the case in study these tensile stresses are not considered by not have a relevant effect on the total force applied on the pile.

3.2.5.6 Gap

When gap occurs, the interface has an elastic behavior being applied the formulation described in the previous point, Eq. 10 and Eq. 11. The displacement u_n and u_t of the interface is controlled by the displacement from the soil. The stiffness of the interface K_s and K_n will remain unchanged since their properties are related to the properties of the interface and to the virtual thickness. It is possible to conclude that will have a direct relation between the increases of the displacement and the increases of the normal and shear stress.

4 2-D ANALYSIS OF A SINGLE PILE

Results from 2-D, plain strain FE analysis is presented in this section. The idealized model and the mesh generation is first shown followed by the interface modeling, influence of depth, soil displacements and influence of "roughness" of the interface. After that, a parametric study is presented fallowed by the conclusions.

4.1 Idealized model in 2-D

For better represent the soil behavior, a model based in the model presented by Chaoui et al. (1994) were studied, where the soil flow around a stiff pile is modeled by imposing an uniform displacement on both sides of the model and the boundary conditions are vertical fixed above and below (Fig. 4.1). Because of symmetry only half of the problem was considered.

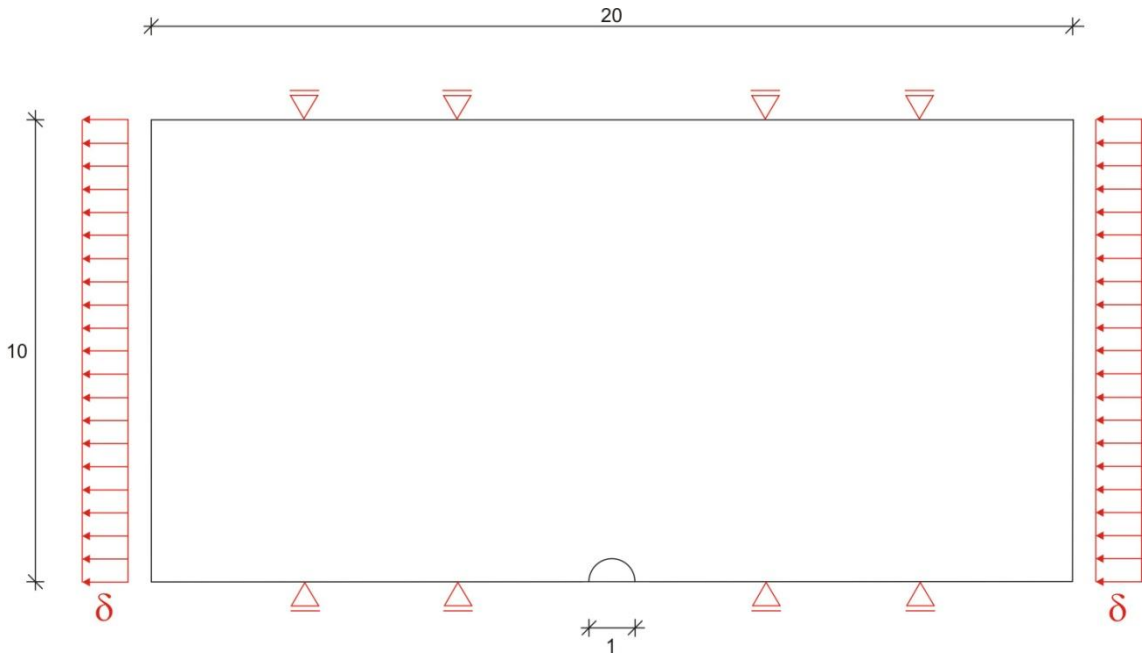

Fig. 4.1 - Developed model in 2-D

This model consider only interface elements around the pile, assuming the fixed concrete-soil interface, due to the big stiffness of the pile($E=32x10^6$ kN/m^2). The

interface soil-soil is considered free and the nodes of the pile are considered as fixed.

A value of 10D (D - diameter of the pile) from the center of the pile is used for the boundaries of the model, in order to prevent any influence of the boundary in the results. This value is proved as correct by Chen (2002).

In order to confirm the viability of the model some calculations were carried out. Fig. 4.2 shows the magnitude of the displacements along the axis of symmetry. The question to be answered is when a displacement is applied in the right boundary, which displacement is expected in the left boundary. In reality is expectable a lower displacement in the left boundary when the soil is moving ($\delta<\delta_0$). However, this value of displacement in the back of the pile is not known.

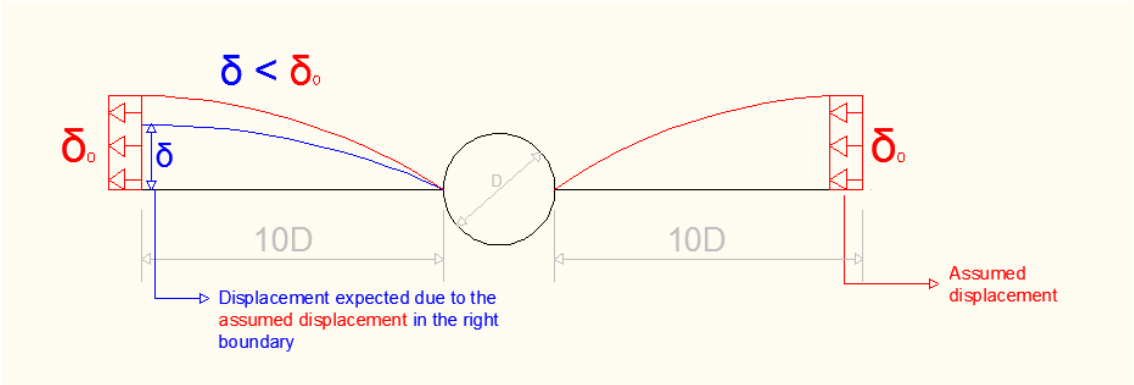

Fig. 4.2 - Representation of the magnitude of displacements along the axis of symmetry

Fig. 4.3 shows the influence of the variation of the displacement in the left boundary in the ultimate force applied at the pile. Fig. 4.3.a) shows the variation of the ultimate force applied on the pile due to the variation of the displacement in the left boundary for a distance of 2D for the left boundary and the rigth boundary remains with a value of 10D. The multiplier factor work as an reductor of the displacement in the left boundary in relation to the right boundary, e.g. δ_{left} = 0,2 δ_{rigth}. It can be seen that with the decrease of the displacement of the left boundary the total force tends to decrease, however, this decrease only start around 0,6 δ_{rigth}. For the case of 10D for both sides of the boundary this curve has a constant value of 617 kN/m for the ultimate force

applied at the pile. This means that for a boundary of 10D, the change of the displacement will not change the value of the ultimate force applied at the pile. This conclusion is also shown in Fig. 4.3.b), where the ultimate force applied at the pile due to the variation of the left boundary for a value of displacement of 0,2 δ_{rigth}. It can be seen that with the increase of the distance for the left boundary the value of the ultimate force applied at the pile increase until reach to a limit value of 10D. This means that after 10D diameters, the boundary has no more influence on the force applied on the pile and the lower displacement in the back of the pile expected in reality can be forgotten. However, the value of the displacement applied on the left boundary has a crucial influence in the gap area generated. With the increase of the displacement also the gap area increases.

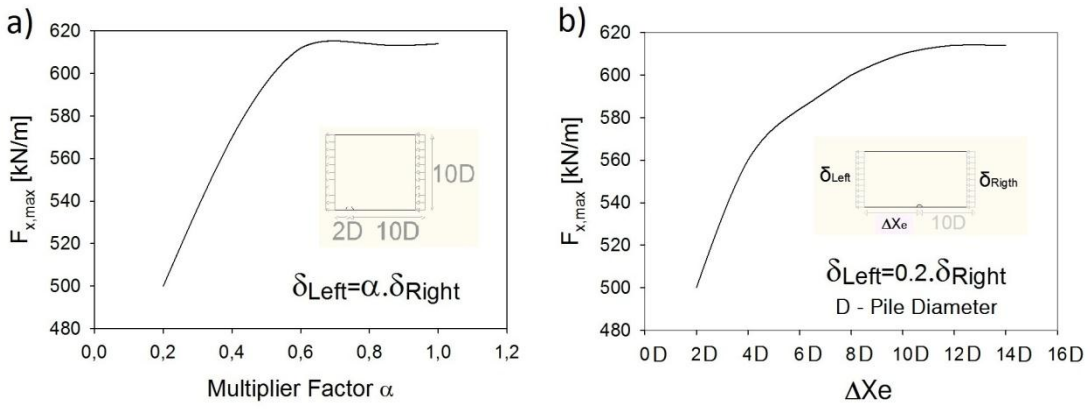

Fig. 4.3 - Ultimate lateral force applied in the pile: a) Displacement applied on the left boundary; and b) distance used in the left boundary for δ_{left} = 0,2 δ_{rigth}

The influence of allow tension on soil was also studied using the "tension cut-off" option from PLAXIS. Sands are not able to resist to any tensile strength unlike the clay, that is able to resist to some tensile strength, however, this value is not known. Was concluded that the effect of reduce the allowed tension on the soil is the same than reduce the displacement on the left boundary, influencing the gap area but not the total force applied at the pile. Fig. 4.4.a shows the deformed mesh when tension is not allow in the soil. Fig. 4.4.b

shows the deformed mesh when tension is allow in the soil. It can be seen that the allowed tension in the soil as influence in the gap area.

During this work, was chosen not allow tension for the interface, although, in reality there is some tension in the moment of separation between the soil and the pile, but is too small to be accounted.

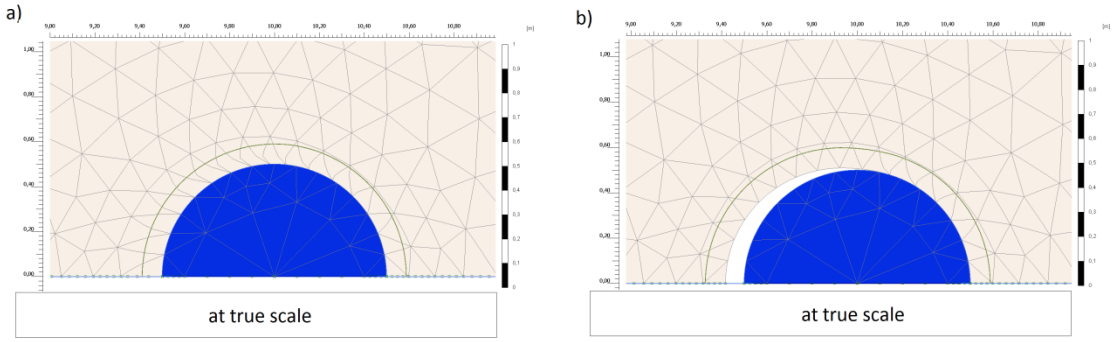

Fig. 4.4 - Deform mesh for the Mohr-Coulomb model: a) with "tension cut-off" criterion applied to the soil; b) without tension cut-off criterion applied to the soil

Fig. 4.5 show the influence of variation of the horizontal boundary on the model. It can be seen in Fig. 4.5 that the variation of the horizontal boundary do not change the ultimate force applied at the pile, except when the boundary is extremely close to the pile (distance of 2D).

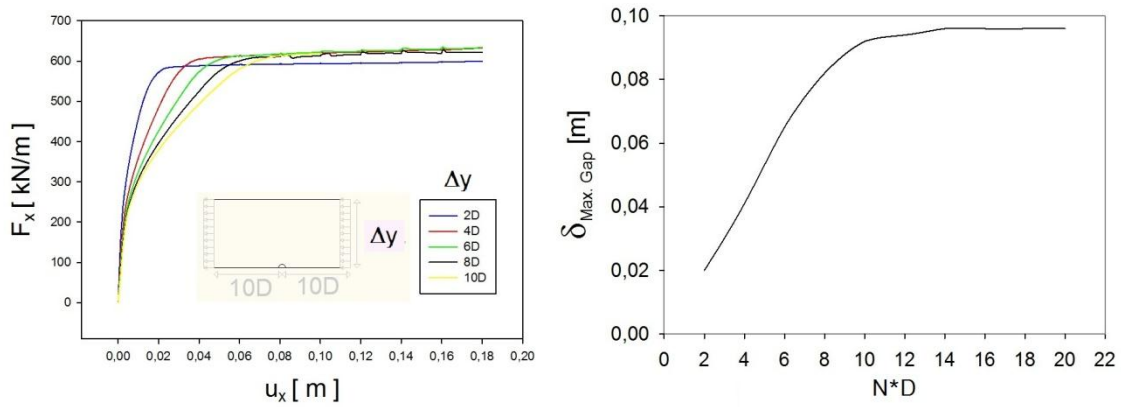

Fig. 4.5 - Distance between pile and lateral boundary side: Total force applied at the pile and maximum gap displacement

4.1.1 Initial Conditions

Until now, the model presented in point 4.1 has been developed considering the section in the surface of the soil, which means that no initial stress are generated due to the weight of the soil.

With this model, it is possible to consider the influence of depth in a 2-D model. To apply the initial conditions in the original model, a system of 3 steps is used:

1. In the first step an additional layer of soil is add and the initial stresses are generated. For this soil is used a linear elastic material with self-weigh of 20 kN/m^3 to provide a gradual increase of the stress constant in both directions. For the layer where is intended the stress field, is used a material without self-weigh but with the parameter K_0 (K_0=σh/σv) set to 1, to provide the same stress in the entire field in both directions (Fig. 4.6.a);
2. In the second step the added layer is removed and the boundary conditions are redefined (Fig. 4.6.b);
3. In the third step the materials are changed for the materials that represent correctly the behavior of the concrete and soil (Fig. 4.6.c).

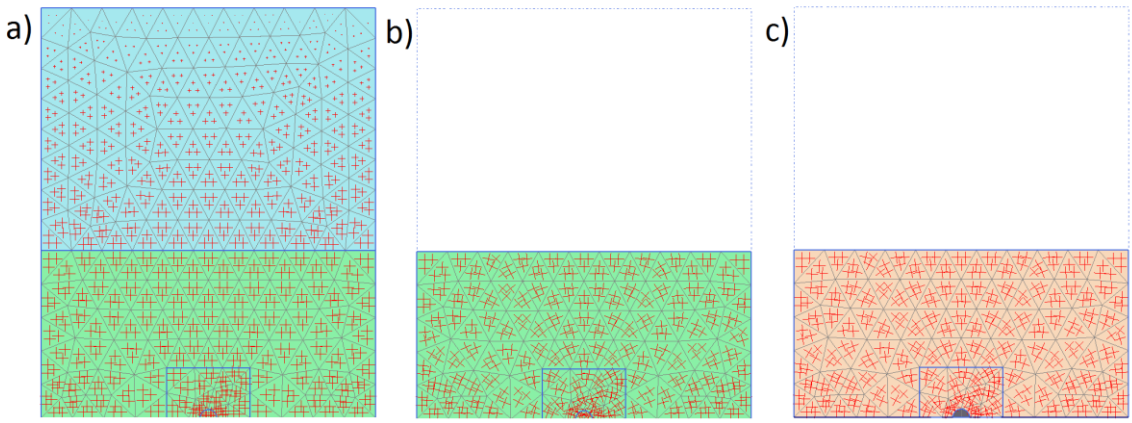

Fig. 4.6 - Process for the implementation of initial conditions

However, this is a 2-D model and has some limitations. The vertical movement of the soil expected in the firsts meters of depth is not take into account. Fig.

4.7 shows the way as the model simulates the influence of depth in terms of vertical and horizontal displacement. This effect has a major importance in calculations for small depths, once that for bigger depths the vertical movement of the soil is negligible due to the gravity effect. In this way, it is expectable to get larger values then in reality of normal stress for small depths.

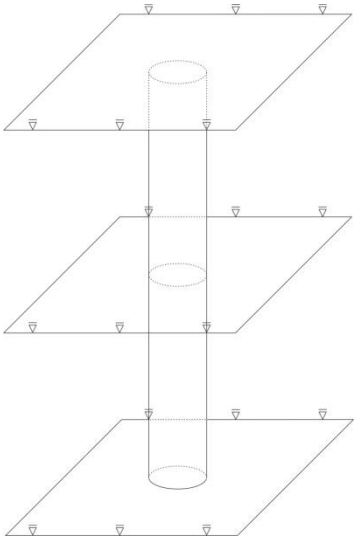

Fig. 4.7 - Illustration of the vertical conditions used by the model simulates the effect of depth

4.2 Selection of soil parameterss

Many previous studies, for example Poulos and Davis (1980) and Chen (1994), have found that, besides the correct estimation of the lateral soil movements, a good prediction of the lateral force F_x depends on an appropriate selection of soil Youngs´s modulus E and the undrained shear strength c_u. Some guidelines are briefly described below for the selection of these parameters.

4.2.1 Young's Modulus E

Young's modulus E may be assessed on the basis of previous laboratory or in-situ test data, such as SPT or CPT. Poulos (1995) develop a series of

laboratory tests for horizontal movements of soils and present the values of $150C_u$ to $400C_u$ for clays.

4.2.2 Undrained Cohesion c_u

Several authors presented different values to the c_u, some of them are presented inTab. 2:

Soil type	Undrained cohesion c_u	Reference
Normally consolidated clay	0 to 20 kN/m^2	Ilyas et al. (2004)
Soft to medium stiff clay	25 to 50 kN/m^2	Rollins et al. (1998)
Stiff over consolidated clay	70 to 180 kN/m^2	Brown et al. (1987)

Tab. 2 - Results obtained with static lateral tests for values of c_u

4.3 Mesh generation

For the mesh generation is used the option "Mesh Generation" and to refine the mesh is used the "Global Refinement" and "Local Refinement". First, a preliminary analysis has been performed using a relatively coarse mesh. This analysis is used to check if the model is large enough and to see where stress concentrations and large deformation gradients occurs. It was observed that the area close to the pile concentrate the most important stress and deformation. To create efficiently a detailed finite element mesh, an area with 5x3 m around the pile has been refined using the option "Refine Cluster" Fig. 4.8.

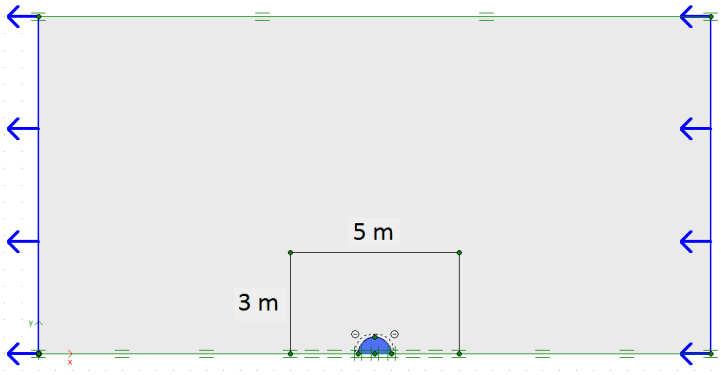

Fig. 4.8 - Adapted model with detailed area

It is presented in Fig. 4.9 the mesh used in the calculation, with 1124 elements. The effect of the Global Refinement was studied and presented in graph form (Fig. 4.10). For the study of the local refinement, very coarse mesh were used as a start point. The point in study is situated 0,2 [m] above the soil pile interface in the direction of middle of the pile. It is possible to conclude with this study that for a boundary with 10D, between 3 and 4 refinements is enough to have a good precision. More than this will result in a mesh too fine and in an increase of computation time without relevant benefice.

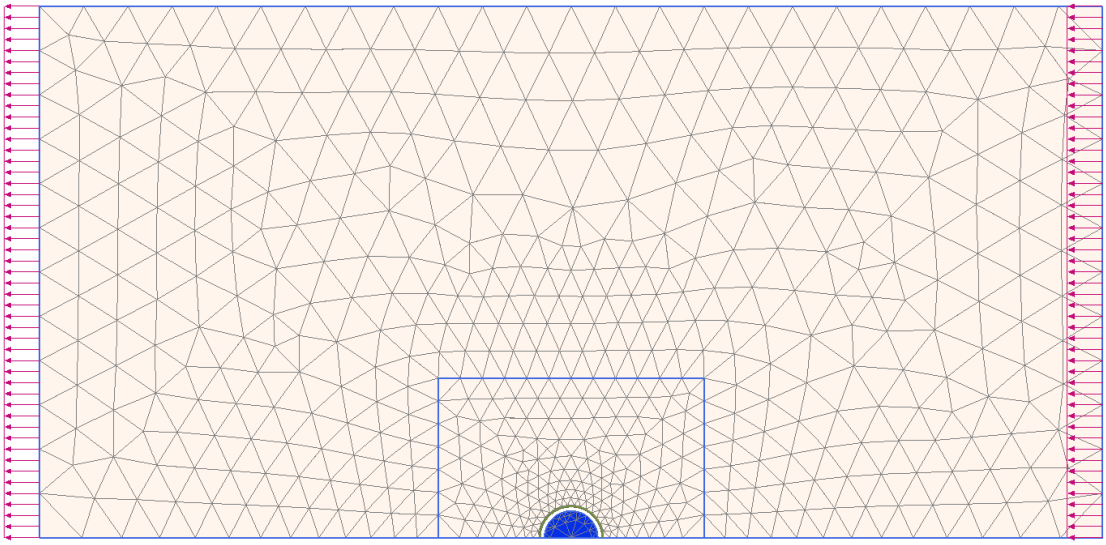

Fig. 4.9 - Composition of the mesh used for calculation

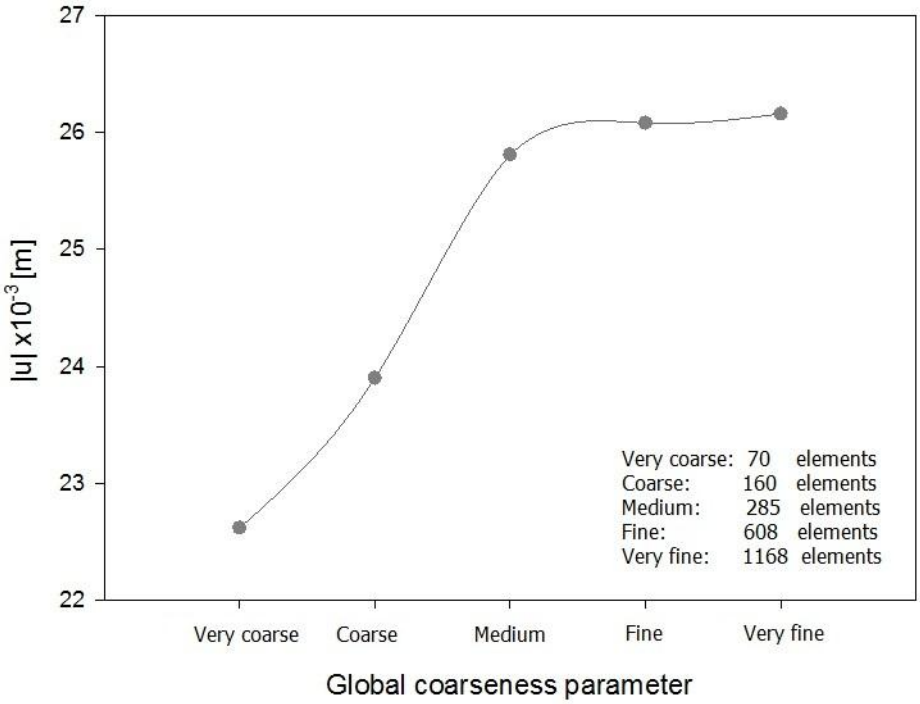

Fig. 4.10 - Study of the influence of the global refinement

4.4 Interface

One of the main problems in modeling the flow of the soil around the pile is the soil-pile interaction and the stress distribution around the pile. The objective of this point is show the main differences in considering different constitutive models and different drainage type for the interface and try to reach a conclusion about which is the best option. For that is used four different approaches to calculation: Mohr-Coulomb constitutive model for soil without the use of interface; linear elastic constitutive model for the soil and interface; Mohr-Coulomb constitutive model using undrained conditions for the soil and interface; and Mohr-Coulomb constitutive model using undrained conditions for the soil and drained conditions for the interface. The results presented below are show for a displacement of 20 cm at both boundaries, under the conditions shown. In all the cases, were considered the soil in undrained conditions, using

the option in PLAXIS "Undrained C" which effects are explain in point 3.2.3. The effects of the initial stress were not taken into account.

4.4.1 Without interface

Some authors, as Van Langen (1991) and Miao et al. (2005), reported the importance of a pre-analysis using a model without interface. The interface stiffness K_s and K_n should be chosen such that the initial slopes of load-displacement curves closely resemble those which are obtained without the use of interfaces (Van Langen, 1991).

The plastic points represent a powerful tool to predict the behavior of the soil around the pile. The Mohr-Coulomb points represent the stress points where the coulomb criterion is activate and the tension cut-off points represent the stress points where the tension cut-off criterion is applied. The images showed in Fig. 4.11 make possible to conclude that in the back of the pile a gap will occurs due to the tension cut-off points and in the front of the pile a slip will occurs due to the Mohr-Coulomb points.

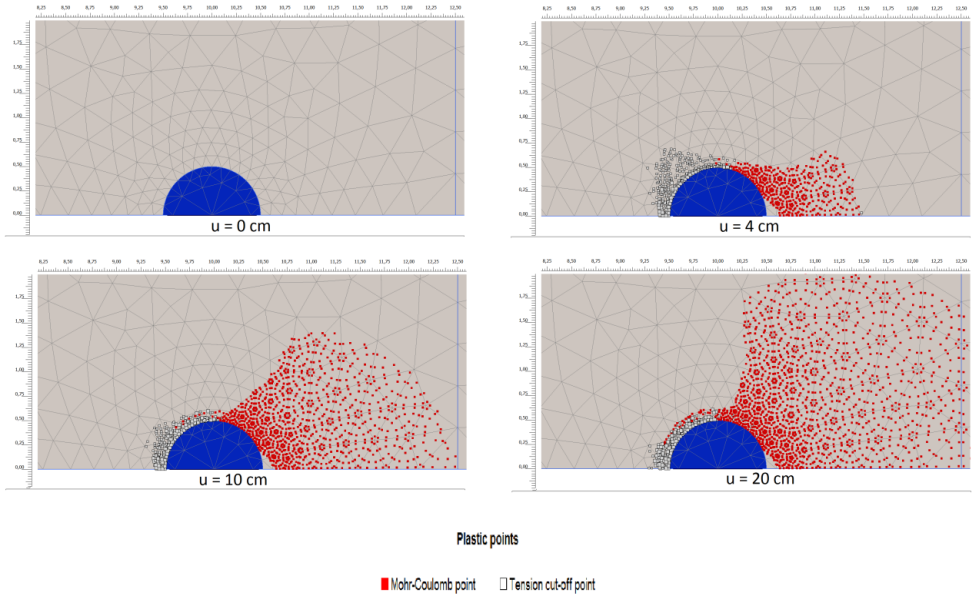

Fig. 4.11 - Plastic points for a model without interface and constant displacement in both boundaries of 0, 4, 10 and 20 [cm]

One of the vantages of this model is that there is no influence of the interface in the behavior of the soil, what give a better idea about the real behavior of the soil around the pile, having in consideration the area immediately after the link between the two materials.

4.4.2 Interface using the linear elastic model

In this point is used the linear elastic constitutive model for the soil and for the interface. The results for the linear elastic constitutive model shows that the behavior of the soil and the interaction soil/structure is not possible to model adequately. The linear elastic is based on Hooke's law, involving two basic elastic parameters (Young's Modulus E and Poisson's Ratio ν), leading to a linear behavior of soil, with a direct relationship between force and total displacement (Fig. 4.12), which does not reflect the reality.

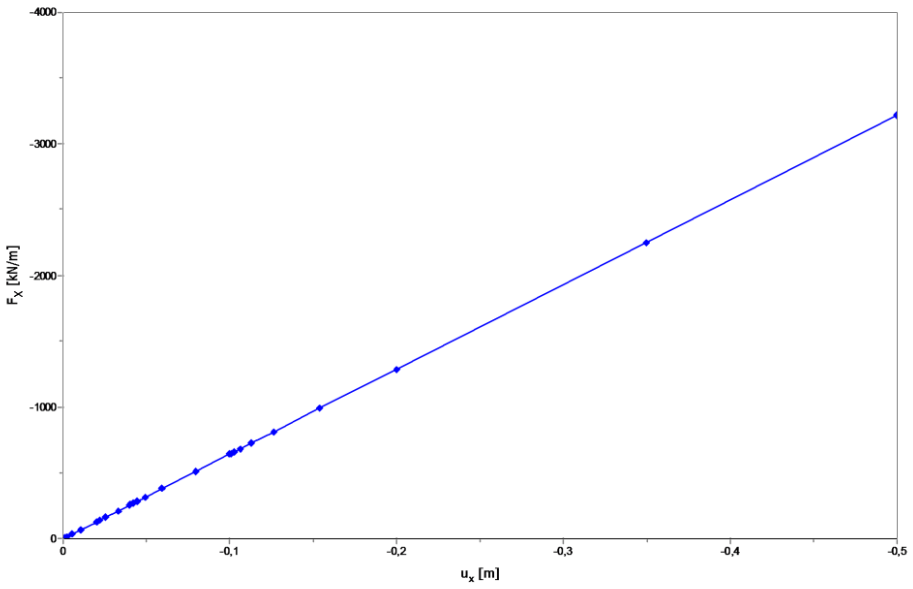

Fig. 4.12 - Horizontal force - displacement graph for the Linear Elastic model

However, this model gives the first impression about the expectable behavior of the shear and normal stress diagram, with maximum compression in the front of the pile (180º), maximum traction in the back of the pile (0º) and maximum shear stress in the middle (90º) (Fig. 4.13).

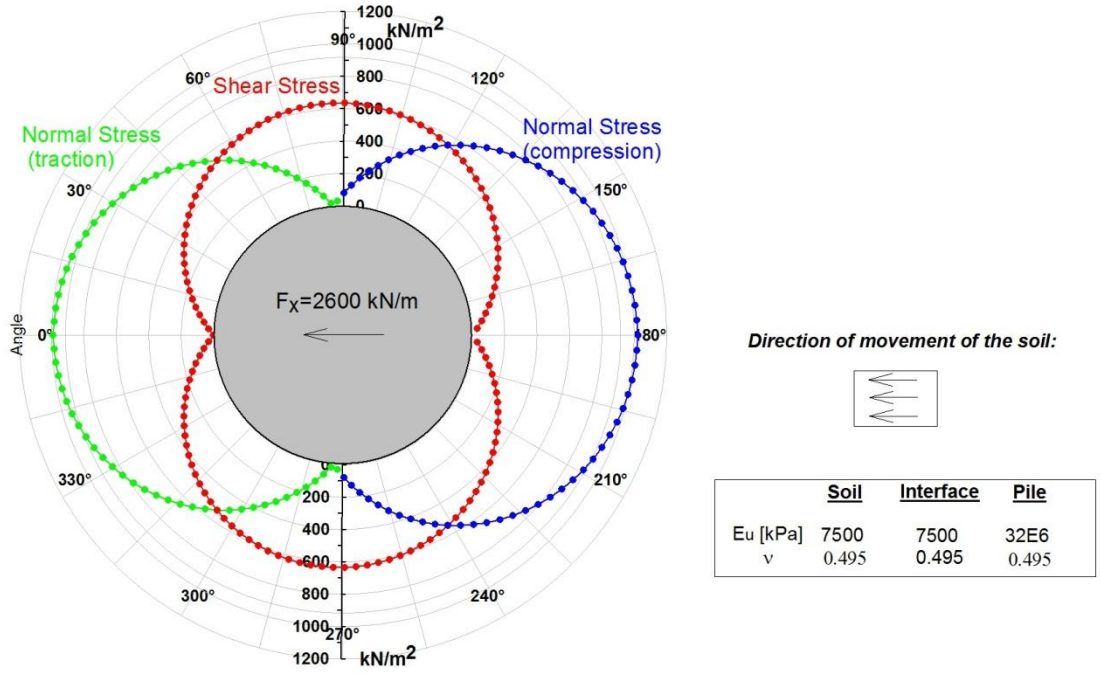

Fig. 4.13 - Normal and shear stress diagram for the Linear Elastic model

The limitations of this model are, as referred before, the elastic behavior based in two basic parameters, Young's modulus E and Poisson's ratio ν, and the option "tension cut-off" is not available for this constitutive model, what means that it will have tension on the back of the pile, which doesn't correspond to the reality. The shear stress diagram is also not realistic, however, better explanation about this behavior is given in the next point (4.4.3). Fig. 4.14 present the deformed mesh for the linear elastic model, with gap in the back of the pile.

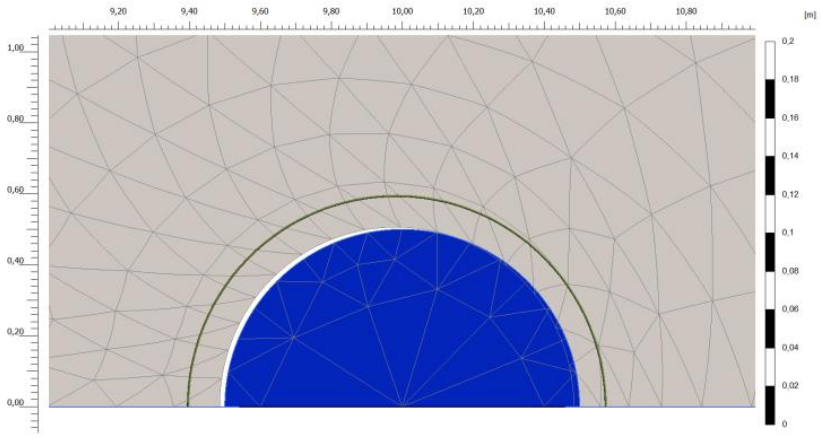

Fig. 4.14 - Deformed mesh for the Linear Elastic model

4.4.3 Interface using the Mohr-Coulomb model

It is presented in this point the main differences and characteristics between consider the interface in drained and undrained conditions, using the Mohr-Coulomb model.

4.4.3.1 Undrained conditions for the interface

In this point, the Coulomb criterion is used to distinguish between elastic behavior (gap and slip) and plastic behavior (only slip). As previously mentioned, for this calculation the soil and the interface in undrained conditions were considered using the "Undrained C" from PLAXIS, with undrained cohesion c_u set to 50 [kN/m^2].

For the modeling of this problem two materials were used, one for the soil and the other for the interface. The materials properties are the same, in order to simulate a total "roughness" between the soil and the pile, only differing the option "tension cut off".

This constitutive model leads to an incorrect shear stress diagram in the zone where gap occurs. This phenomenon is show in Fig. 4.15, where it is possible to see that between 0º and 90º and between 270º and 360º degrees, where gap

occurs, the shear stress diagram is not zero. This phenomenon is explained in point 5.2. The normal stress diagram presents a correct behavior, with the maximum stress in the front of the pile and decreasing this value until reach to zero where gap occurs. It is important note that the normal stress diagram has some bumps in the area between the front and the middle of the pile. This is an important limitation of PLAXIS and this phenomenon is due to excess of deformation of the elements.

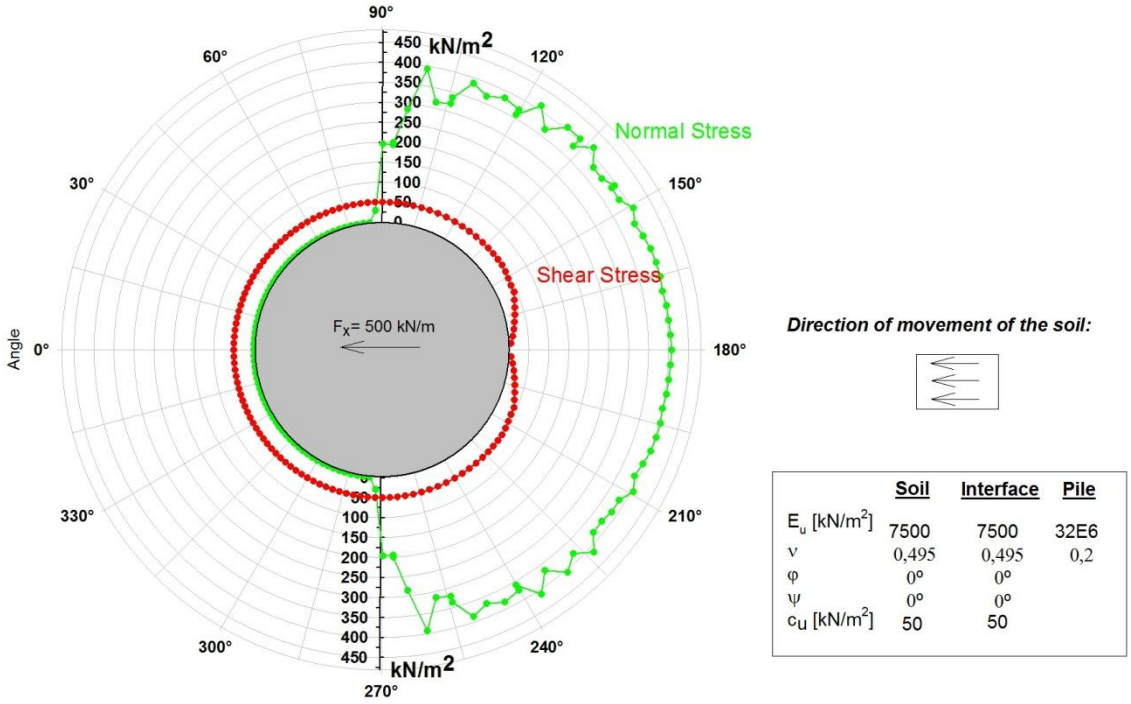

Fig. 4.15 - Normal and shear stress diagram for the Mohr-Coulomb model (Undrained C)

Fig. 4.16 show the horizontal force - displacements for half pile. It can be seen that the curve as an different behavior comparing to the linear elastic model. The curve starts with an elastic behavior for small displacements, change for nonlinear behavior in intermediate values and finish with the ultimate force applied at the pile for large deformation, which in this case is 330 kN/m^2. This behavior will be better explained in point 4.8. The development of this curve is directly related with the Coulomb criterion. For small displacements, the coulomb criterion is not applied in any stress point, so the behavior is linear elastic. For intermediate values, the Coulomb criterion is applied in some stress

point and the behavior is no more linear. For big displacements all the stress point that contribute for the generation of stress in the interface has the Coulomb criterion applied what makes the ultimate force be reached.

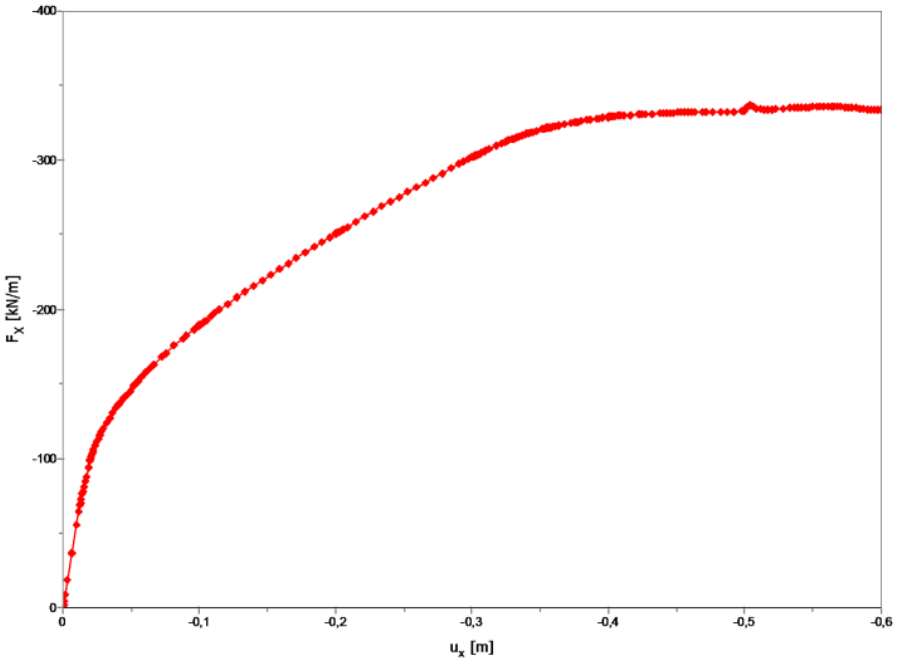

Fig. 4.16 - Force displacement curve for the Mohr-Coulomb model in undrained conditions

4.4.3.2 Drained conditions for the interface

For this calculation, the soil in undrained conditions with undrained cohesion c_u set to 50 kN/m^2 were considered. For the interface, drained conditions with friction angle φ set to 22,6º (Miao et al. (2005)) and cohesion c set to 0 kN/m^2 were considered. For the soil and for the interface the Young's Modulus were set to 1000 kN/m^2 due to "soil collapse" error during the calculation with Young's Modulus set to 7500 kN/m^2.

Taking into account the Mohr-Coulomb yield function f(t) presented before, it is possible to conclude with this constitutive model that if drained conditions are selected for the interface and the cohesion c is set to zero, when the Coulomb

criterion is applied, the Coulomb yield function is controlled only by the normal stress and the friction angle. It is possible to seen in Fig. 4.17 that the shear stress diagram presents a correct value (equal to zero) in the back of the pile and in the front of the pile, in the zone where the Coulomb criterion is applied, the value of the shear stress diagram is totally controlled by the normal stress and by the friction angle φ.

Despite the shear stress diagram has the expectable form, the way how this form is archived do not represent correctly the reality, do not enable a correct control on the "roughness" of the interface and bring some numerical problem during the calculation.

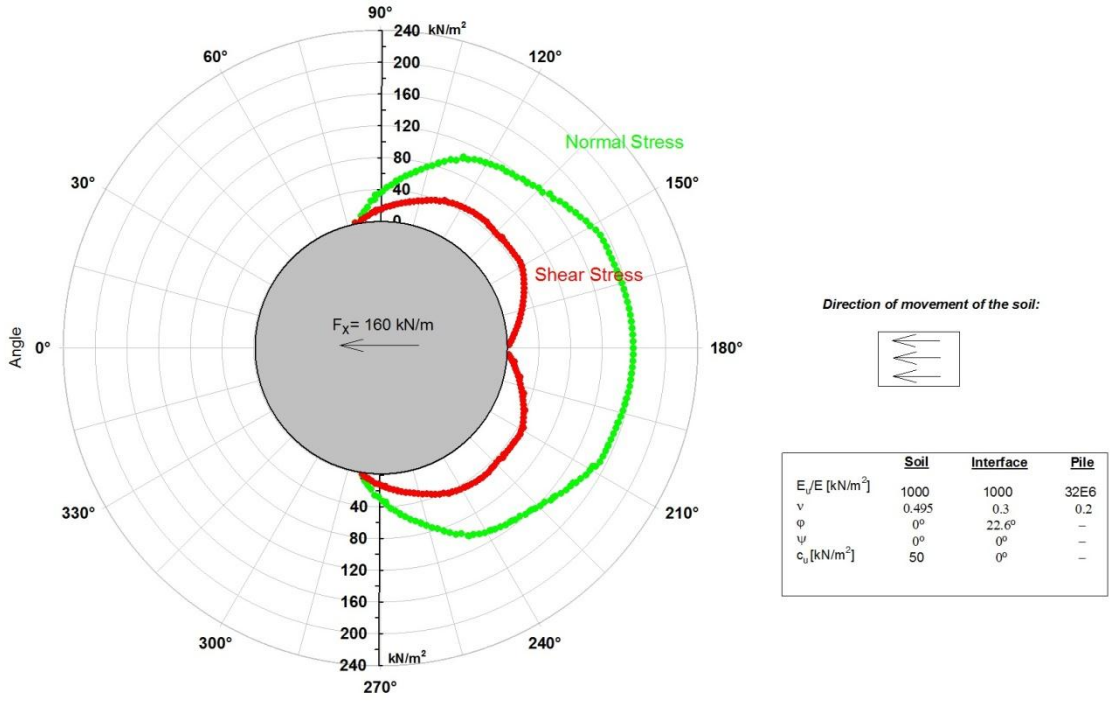

Fig. 4.17 - Normal and shear stress diagram for the Mohr-Coulomb model - Drained conditions for the interface

4.4.4 Conclusion

As a conclusion of this point, it was found major difficulties in obtaining an adequate shear stress diagram. The shear stress diagram in the interface when gap occurs is one topic that is better studied in chapter 5. There is some ways

to try to approximate the diagram to the expected, like with drained conditions for the interface and setting the cohesion to zero, but this way do not allow a control on the "roughness" of the interface and bring numerical problems during the calculation. The shear stress diagram depends always from the values assigned for the interface. The shear stress diagram presented is relative to the interface elements and not to the pile surface.

The normal stress is represented correctly when the "tension cut-off" criterion is applied to the interface, with the maximum normal stress in the front of the pile and zero in the zone where gap occurs. However, exist some bumps in the diagrams, especially in the Mohr-Coulomb model in undrained conditions. This behavior happens due to excess of deformation of the mesh, especially in the zone between 90º and 135º (Fig. 4.15), due to the fact that is in this zone where the biggest deformation happens. PLAXIS use the update Lagrange - Finite Element Method and with the increase of deformation is expected that this bumps appears. Therefore, only is possible get correct results for small deformation.

For a correct modeling of this problem, the tension cut-off criterion should be used for the interface.

Taking into account the conclusions presented before, was chose continue the study using the same drainage type for the soil and for the interface (Undrained C) for being the option that offer better conditions in term of computation time and control in the "roughness" of the interface.

4.5 Influence of depth

In this point, the influence of the variation of depth on the ultimate pressure applied on the pile, and in the shear and normal stress diagram is discussed. First is done a comparison of the results obtained with the ultimate pressure applied on the pile with the results obtained by other authors (Matlock (1970)

and Pan et al. (2002)), then, the influence of depth in the normal and shear stress is presented.

4.5.1 Validation of the model

In order to compare the model presented in the point 4.1.1- Initial Conditions, to simulate the influence of the initial stress in the pile, is carried out in this point a study of the ultimate soil pressures variation with depth and compared with the results of Matlock (1970) and the 3-D analysis of Pan et al. (2002).

It is considered for the calculation a single stiff pile in soft clay with $E=350c_u$ (c_u=7.62 kPa), Poisson's ratio of the soil was assumed to be 0,495, with update mesh calculation, R_{inter}=1, allowing tension in the soil. The Undrained (B) from PLAXIS were used in this calculations to present in the first meters of depth values more similar to the expected. Fig. 4.18 illustrate the normalized P-u curves for a stiff pile. The computed maximum ultimate soil pressures were $12.7c_u$ considering a stiff pile. This pressure is close to the values proposed by various researchers for active piles e.g. 9 c_u recommended by Broms, 8 c_u by Viggiani, 10.5 by De Beer and Wallaysand, 11.4 c_u by Chen and 11.95 c_u by Bransby and Springman. The reason for this difference is because a 2-D analysis has some limitations, as the vertical movement of the soil and the movement of the pile, and may not properly simulate the real behavior when piles are subjected to lateral movements.

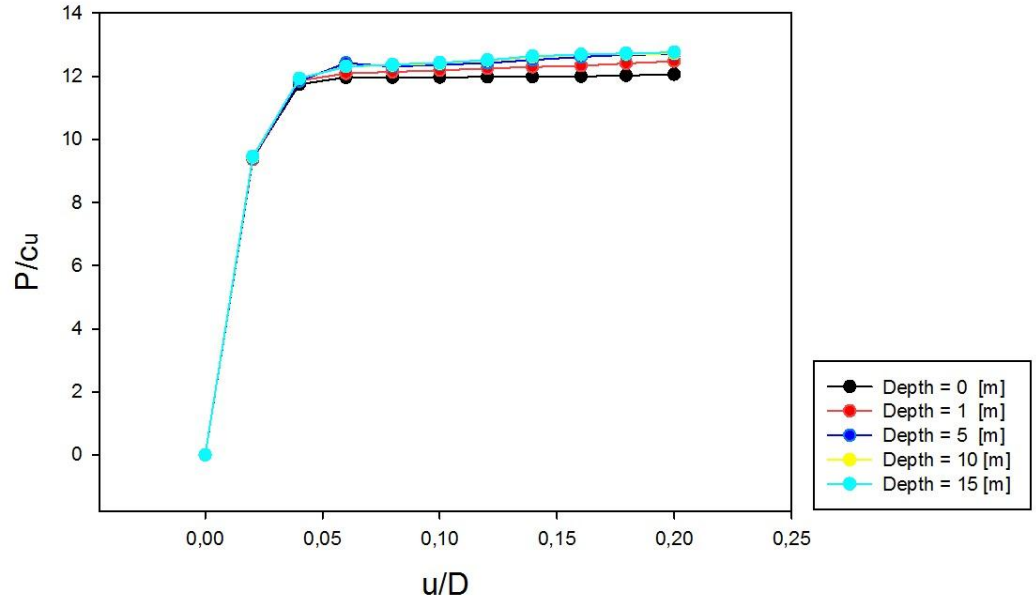

Fig. 4.18 - Normalized P-u curves

Fig. 4.19 shows the variations of the ultimate soil pressures with depth for a stiff pile, together with the plots for passive piles in soft clay proposed by Matlock (1970) and Pan et al. (2002). Matlock (1970) determine the ultimate soil pressure P as a smaller of the values given by the equations below:

$$P = \left[3 + \left(\frac{\gamma'}{Su}\right).z + \left(\frac{0{,}5}{D}\right).z\right].Su \qquad \text{Eq. 26}$$

$$P = 9Su \qquad \text{Eq. 27}$$

where γ' is the average effective unit weight and z is the depth from the ground surface. Pan et al. (2002) develop a 3-D analysis using the finite element program ABAQUS with the von Mises constitutive model.

The strain-softening behavior observed close to the ground surface in Pan et al. (2002) and Matlock (1970) is likely due to the heave of the soil in front of the pile. This explanation is not valid for the results computed in PLAXIS, once the model in 2-D do not take into account the vertical movement of the soil.

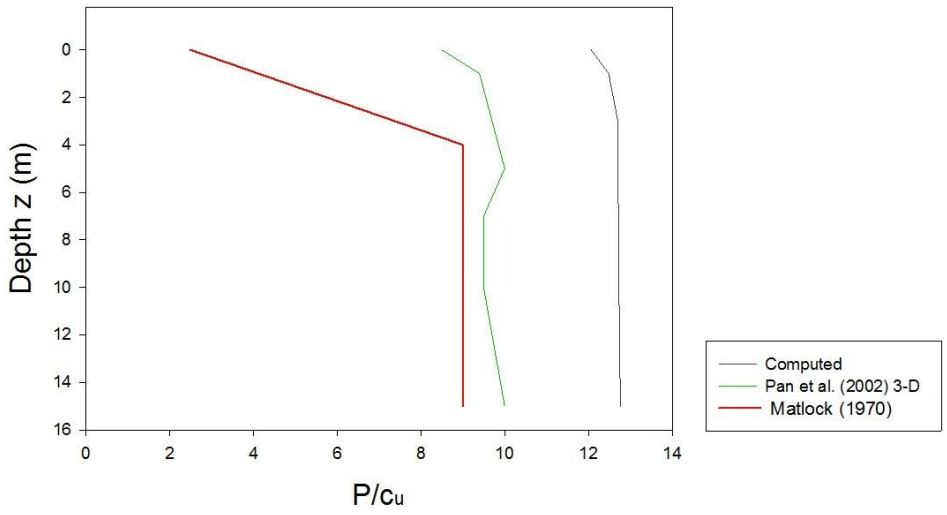

Fig. 4.19 - Comparison of results obtained with the results presented by Matlock(1970) and Pan et al. (2002) for variation of ultimate pressure with depth considering a stiff pile

4.5.2 Influence of depth in the normal stress

Fig. 4.20 shows the variation of the normal stress diagram with the variation of depth, for a displacement of 20 cm in both boundaries (left and right). With the increase of depth, the normal stress diagram is affected: the normal stress is increasing in the front and in the back of the pile. The increase of the normal stress in the back of the pile observed in the Fig. 4.20 for z = 10 m shows that with the increase of depth the gap in the back of the pile occurs increasingly later. This effect is better explained in Fig. 4.21. For 20 cm of displacement, only for a depth of z=10 m the ultimate pressure is achieve. It is possible to conclude that with the increase of depth, it is needed less displacement to archive the ultimate force.

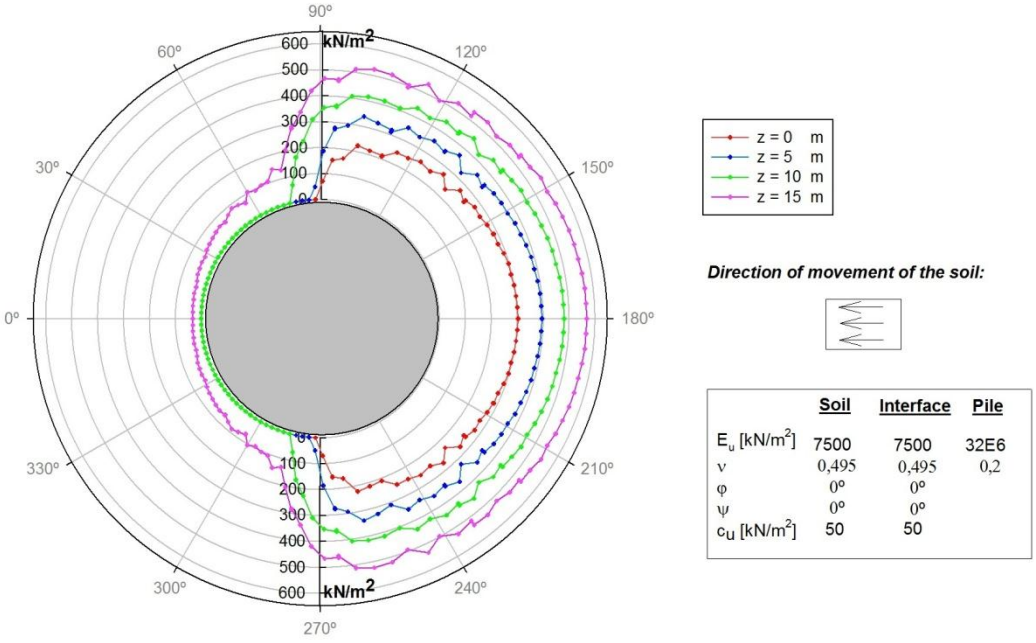

Fig. 4.20 - Normal stress diagram for a displacement of 20 cm (variation of depth)

Fig. 4.21 shows the variation of the normal stress diagram for a depth of 10 m due to a uniform displacement of 0, 2, 4 and 10 cm in both boundaries. For a displacement of u=0 cm, the stress is constant around the entire pile and represent the initial state of stress for a depth of 10 m. With the increase of the displacement, the stress decrease in the back of the pile (0º) and increase in the front of the pile (180º) until the stress in the back of the pile reaches to zero and gap occurs.

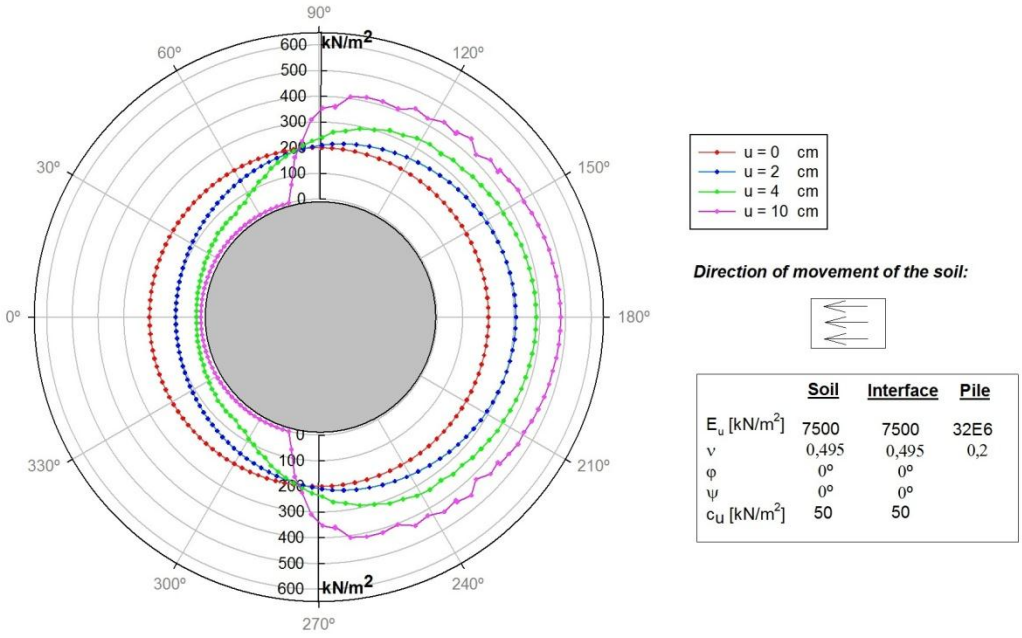

Fig. 4.21 - Normal stress diagram for a depth of 10 m (variation of displacement)

Fig. 4.22 shows typical lateral force-displacement applied in the boundaries behavior of the pile-soil system. The curves shown in Fig. 4.22 are linear at small displacements. The rate of increase of lateral force on the pile decreases at intermediate displacements. Eventually, the reaction force on the pile reaches a peak value and remains unchanged at large displacements when the frictional strength of the soil is fully mobilized.

Also shown in Fig. 4.22 are the effects of initial state of stress on the force-displacement response. It can be seen that variation of depth affects the linear behavior at small displacements increasing with the increase of the depth and the plastic behavior for intermediate displacements rate increase with the increase of the depth. However, the total force remains approximately unchanged, changing only the displacement needed to achieve the ultimate force. With the increase of depth also increase the displacement needed to archive the respective value of ultimate force.

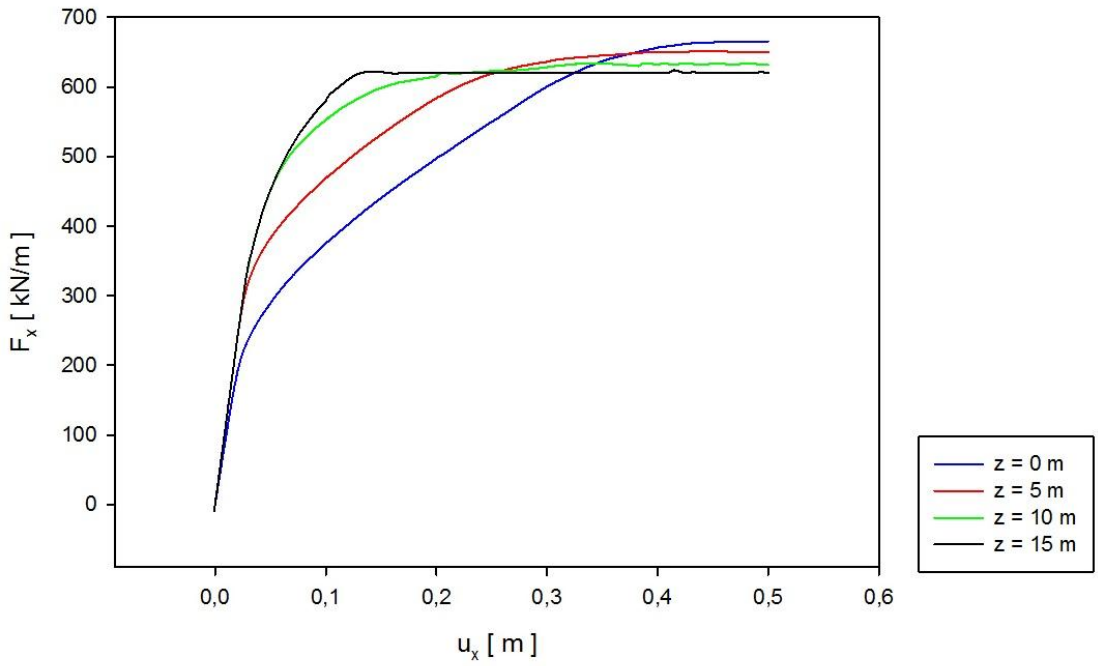

Fig. 4.22 - Lateral force on half piles versus displacement for variation of depth

Fig. 4.23 shows the contribution of the normal and shear stress in the constitution of the lateral force curve for the variation of depth. It can be seen that with the increase of the depth the influence of the normal stress increase and the influence of the shear stress decrease. This phenomenon is due to the increase of the initial stress with the increase of depth.

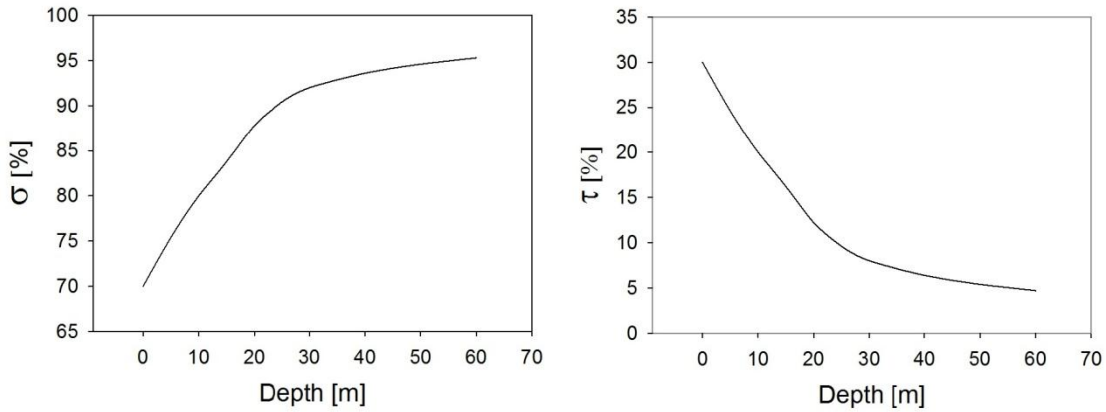

Fig. 4.23 - Contribution of the normal and shear stress in the constitution of the total force due to the variation of depth

4.6 Influence of "roughness" of the interface

The roughness is genetared because the pile surface is marked by irregularities which increase the friction between the pile and the soil. This behavior can not be simulated on PLAXIS. What is possible to do is use the interface elements to increase or decrease the friction between the soil and the pile in order to aproximate the behavior of the interface elements to the real behavior of the interaction pile-soil. Until now, does not exist any program who takes the real roughness into account.

Fig. 4.24 shows typical lateral force-displacement behavior of the pile soil system for a single pile at a sliding depth of 15 m below the ground level. The soil parameters used for the calculation are described in Tab. 3. Is used in this calculation the option of "Undrained C", allowing tension in the soil, a value for R_{inter} of 0.5 for the smooth interface and a value of 1 for the rough interface.

Description	Symbol and Unit	Magnitude
Undrained Young's	E_u kN/m^2	7500
Undrained Poisson's ratio	ν_u	0,495
Undrained cohesion	c_u kN/m^2	50

Tab. 3 - Soil properties used for the influence of roughness study

Also shown in Fig. 4.24 are the effects of interface roughness on the force-displacement response. It can be seen that interface roughness affect the initial stiffness of the f-δ at small displacements and the maximum lateral load on the pile. The rough interface condition yields the largest ultimate lateral force on pile and the smooth interface condition yields the smallest ultimate lateral force on

the pile. This are the expected results, once the "roughness" is bigger, the total friction between the pile and the soil will be bigger also, resulting in a largest ultimate lateral force.

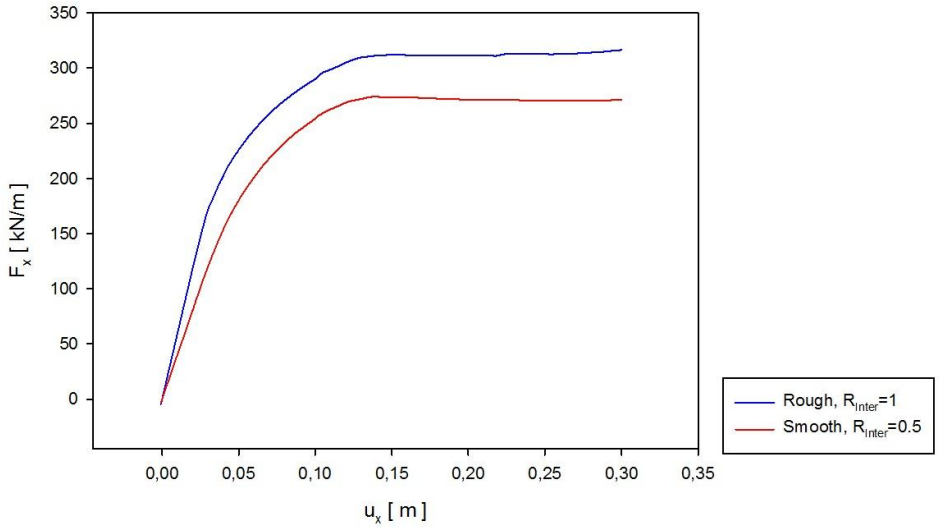

Fig. 4.24 - Lateral forces on pile versus displacement for variation of roughness

4.7 Soil displacements

It is presented in this point the soil behavior for the case in study. It can be seen in Fig. 4.25, Fig. 4.27 and Fig. 4.28 that with the increase of the displacement the soil has tendency to have the largest displacement in the zone close to the middle of the pile. This zone has an oval shape and is not near to the pile due to the friction between the pile and the soil. The largest displacement happens in this zone due to the decrease of the space for the soil move, due to the presence of the pile, causing an increase of velocity. Because of the nearly incompressible behavior of the soil, the displacement in the remote zone from the pile is nearly the same, having a small increase in the left side of the model due to the increase of the velocity in the middle of the model.

Fig. 4.26 shows the ultimate force applied in the pile due to a uniform displacement in both boundaries. The develop of the force-displacement curve as a crucial importance on the displacement field. The ultimate force is reached

for a applied displacement in both boundaries of 0,08 m, what coincide with the appearance of the oval shape in Fig. 4.27. This phenomenon happens because the ultimate force only is reached when the soil is completely mobilized.

It is presented in Fig. 4.29, Fig. 4.30, Fig. 4.31 and Fig. 4.32 the stress points for a uniform displacement in both boundaries of 0,04, 0,06, 0,08 and 0,2 m. It can be seen that in the oval shape where the largest displacement happens, the stress points are not Mohr-Coulomb points (plastic points). It can be also seen that the elements in this area are not very deformed, compared with the elements in the surround area, what explain the absence of Mohr-Coulomb points in this area.

Fig. 4.33 and Fig. 4.34 shows the total displacements u_x for a uniform displacement in both boundaries of 0,06 and 0,1 m. It can be seen that the horizontal displacement (u_x) has the biggest influence in the total displacements |u| in the zone surrounding the pile, once the horizontal displacements in that zone are approximately 2,5 times the vertical displacements, and has the main influence in the generation of the oval shape described before. Fig. 4.35 and Fig. 4.36 shows the total displacements u_y for a uniform displacement in both boundaries of 0,06 and 0,10 m. It can be seen that the vertical displacements has the main influence in the displacements in the front and in the back of the pile.

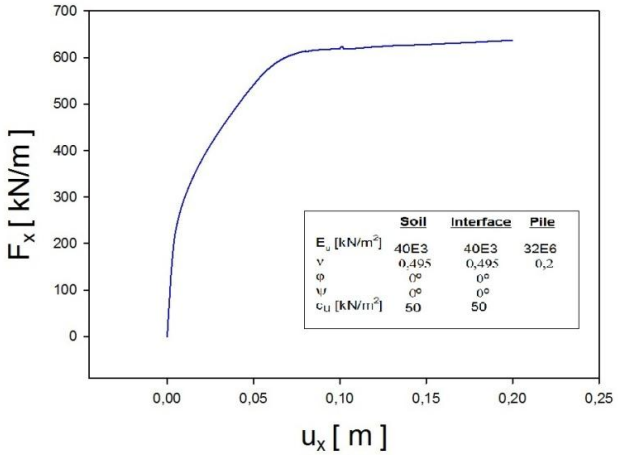

Fig. 4.26 - Horizontal total force applied in the pile

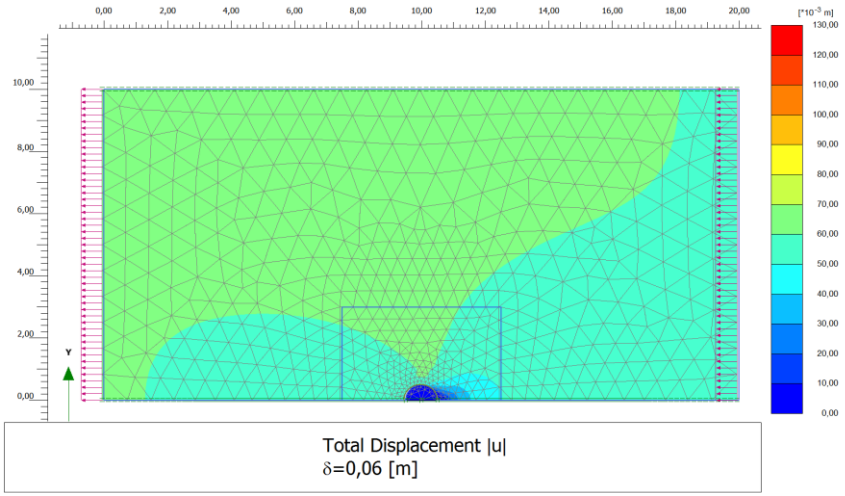

Fig. 4.25 - Total displacement for a uniform displacement in both boundaries of 0,06 m

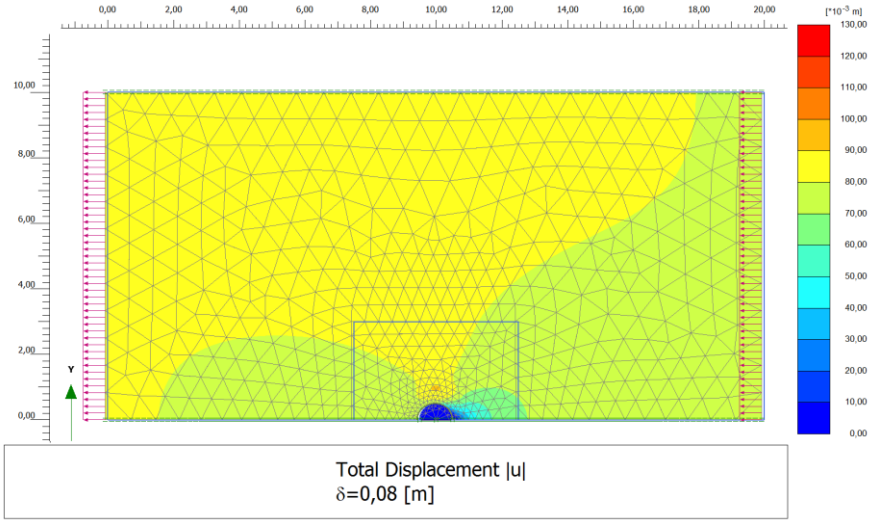

Fig. 4.27 - Total displacement for a uniform displacement in both boundaries of 0.08 m

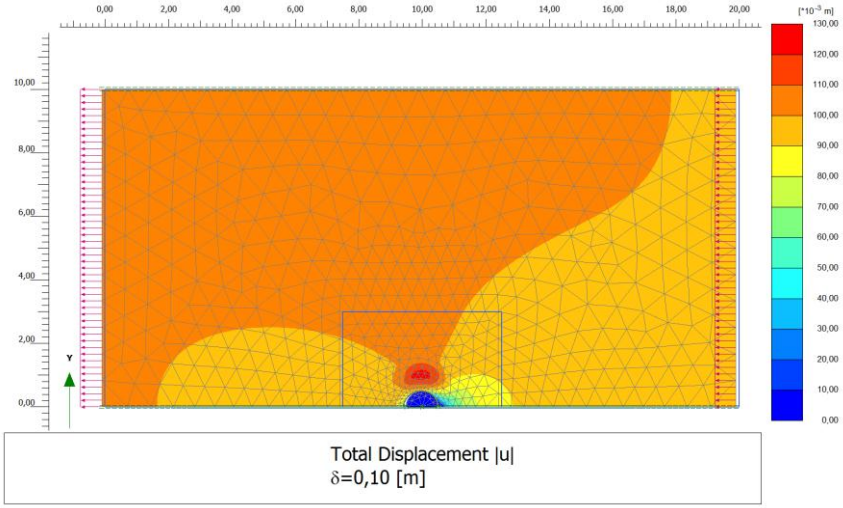

Fig. 4.28 - Total displacement for a uniform displacement in both boundaries of 0.1 m

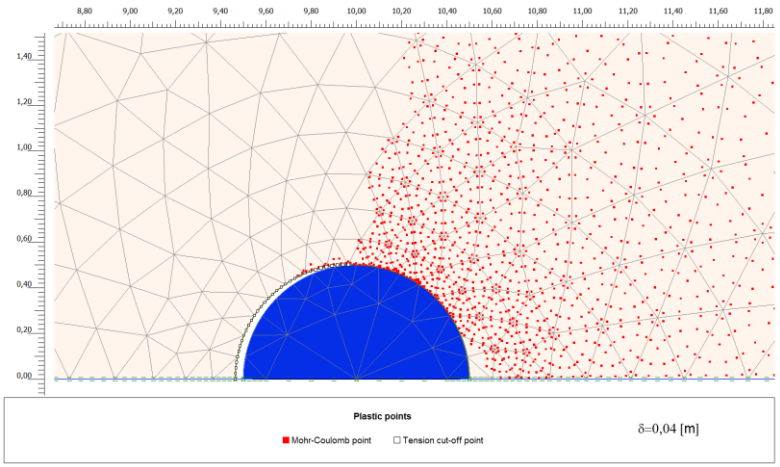

Fig. 4.29 - Plastic points for a displacement in both boundaries of 0,04 m

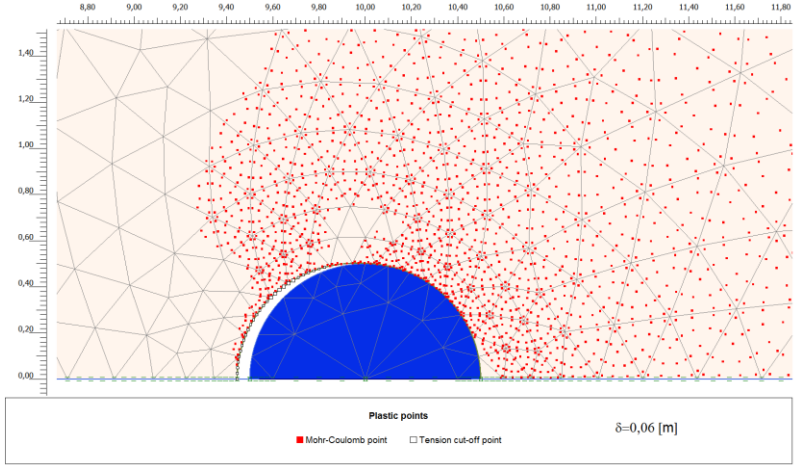

Fig. 4.30 - Plastic points for a uniform displacement in both boundaries of 0,06 m

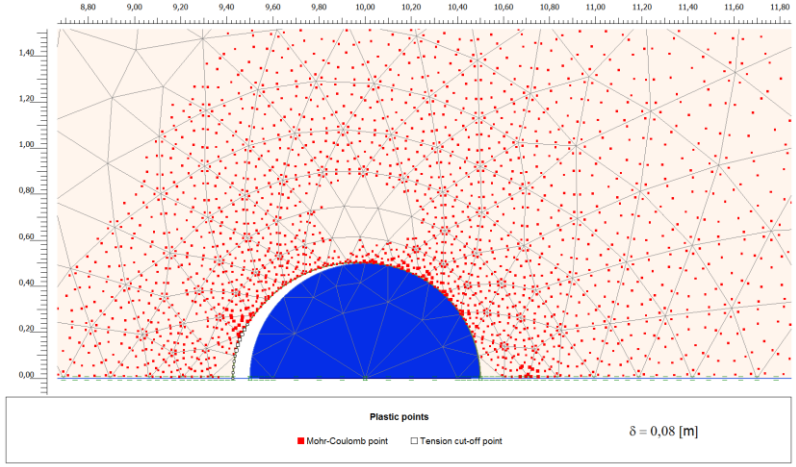

Fig. 4.31 - Plastic points for a displacement in both boundaries of 0,08 m

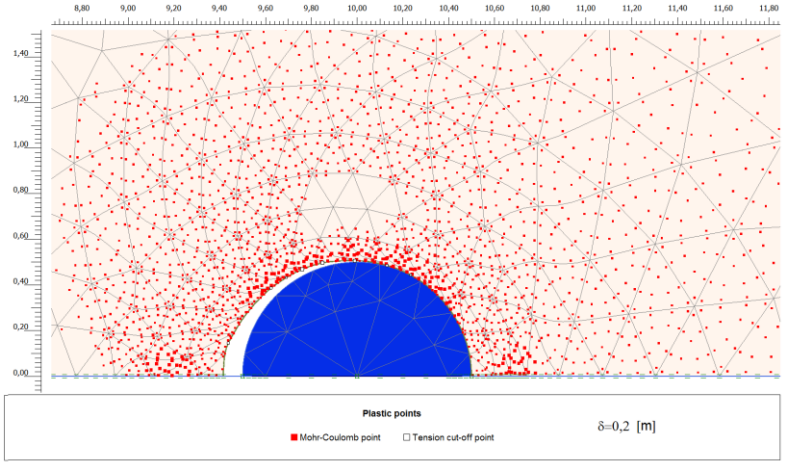

Fig. 4.32 - Plastic points for a displacement in both boundaries of 0,2 m

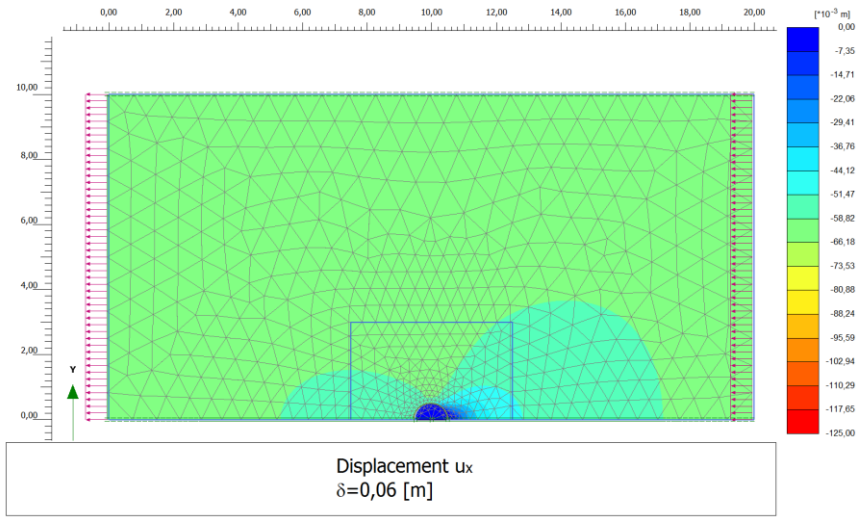

Fig. 4.33 - Displacement ux for a uniform displacement in both boundaries of 0,06 m

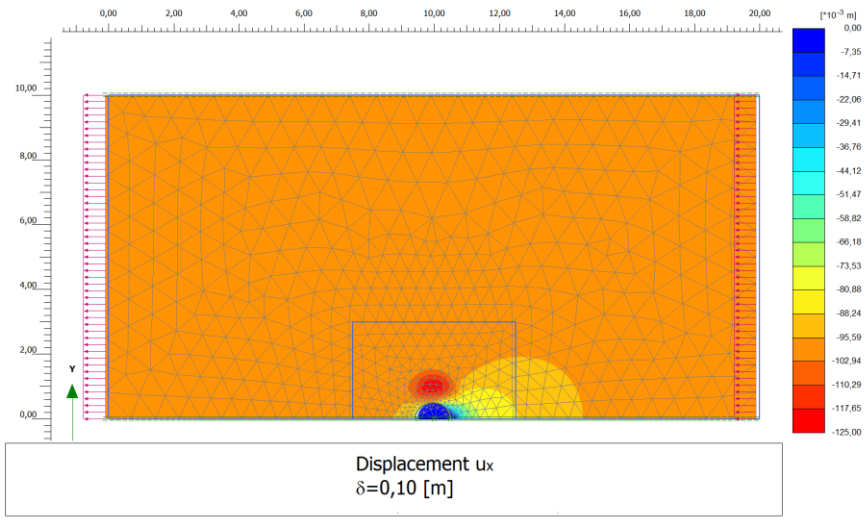

Fig. 4.34 - Displacement ux for a uniform displacement in both boundaries of 0,1 m

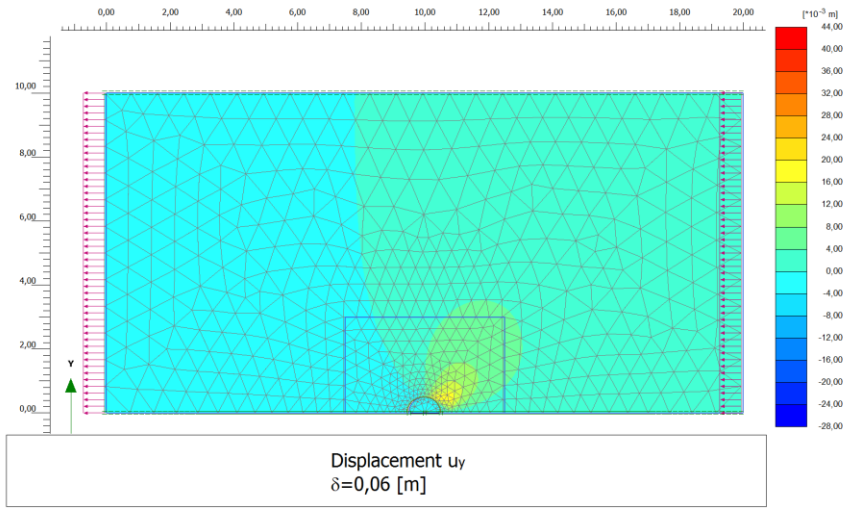

Fig. 4.35 - Displacement uy for a uniform displacement in both boundaries of 0,06 m

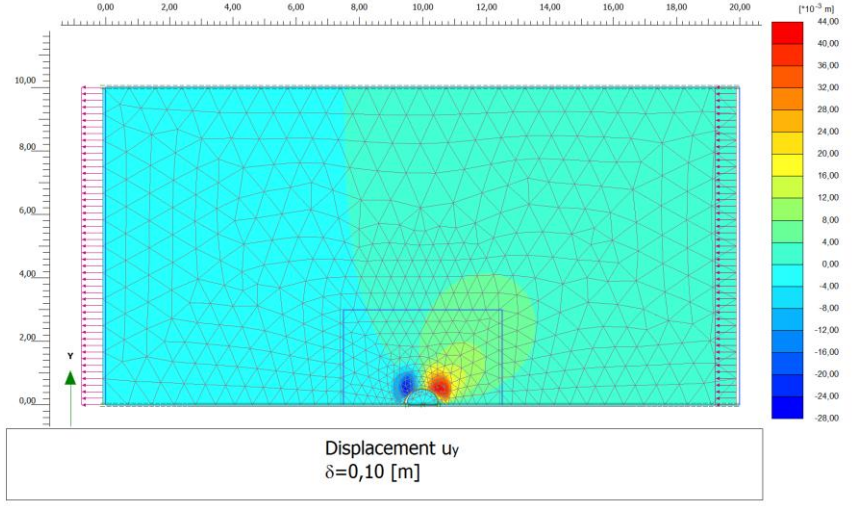

Fig. 4.36 - Displacement uy for a uniform displacement in both boundaries of 0,1 m

4.8 Parametric Study

In this point the influence of undrained cohesion c_u, Undrained Young's modulus E_u, the virtual thickness and the pile diameter on the pile reaction force and on the shear and normal stress are presented. The influence of c_u and E_u is considered in two different situations: in the soil properties; and in the interface properties. The results of normal and shear stress were presented only for a displacement of 2 cm, without initial conditions (depth = 0 m), with the option "Undrained C" and using the parameters and conditions shown. A value of 2 cm is selected because for this value of displacement the diagram is not affected by bumps resulting by excess of deformation of the elements.

4.8.1 Variation of c_u in the interface properties

Fig. 4.37 shows the influence of undrained cohesion on the normal stress diagram for a displacement of 0,02 cm. With the increase of the undrained cohesion, the normal stress decrease until the coulomb criterion is no longer applied. This is possible to see comparing the value for c_u=100 to the value of c_u =50 kN/m^2. For 100 kN/m^2 the Coulomb criterion is no more applied and the value of the normal stress is nearly the same than for c_u=50 kN/m^2.

The influence of undrained cohesion on the reaction force at half pile is shown in Fig. 4.38.a), which shows the f-δ behavior for values of c_u of 10, 30, 50 and 100 kN/m^2. It can be seen that with the increase of the undrained cohesion, the total force as a small increase. This is the expected behavior, once with the increase of undrained cohesion, also the "roughness" of the interface increase causing an increase of friction forces on the interface and increasing the value of the ultimate force.

Fig. 4.38.b) shows the influence of undrained cohesion on the shear stress diagram for a displacement of 0,02 cm. It can be seen that the undrained cohesion has an direct influence on the maximum shear stress. In undrained

conditions, the friction angle is zero causing an direct influence on the Coulomb criterion by the undrained cohesion. While the Coulomb criterion is applied the value of the shear stress is the same as the undrained cohesion. When the Coulomb criterion is not applied the undrained cohesion do not have any influence in the results, e.g. for c_u=100 kN/m^2.

Tab. 4 shows the influence of undrained cohesion on the displacement of the soil. The values of displacement were calculated from the point where the largest gap displacement happens, which in this case is in the back of the pile (0º). It can be seen that with the increase of the undrained cohesion the value of the displacement decrease. This is the expectable behavior, once if the "friction" increases with the increase of the c_u (Fig. 4.38.a) and .b)), the displacement decrease.

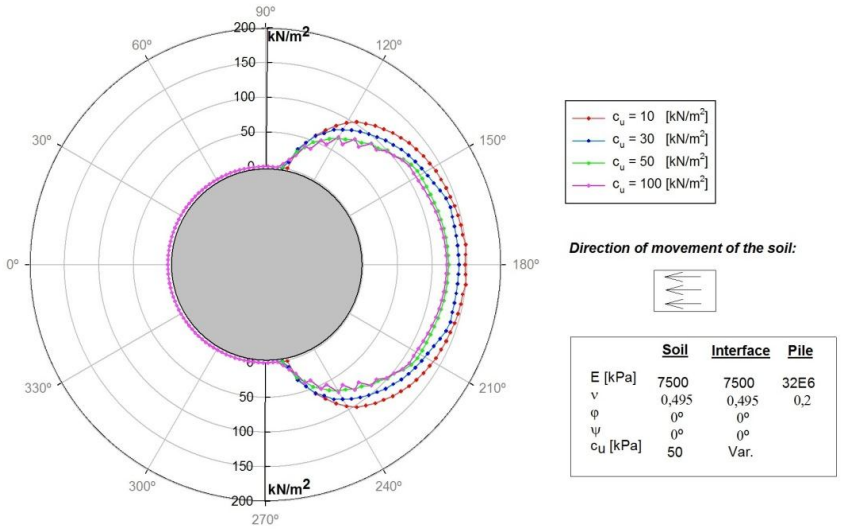

C_u kN/m^2	Displacement m
10	0,0140
30	0,0120
50	0,0103
100	0,0102

Tab. 4 - Displacements for variation of c_u (point 0º)

Fig. 4.37 - Normal stress diagram for variation of c_u in the interface for a displacement of 2 cm

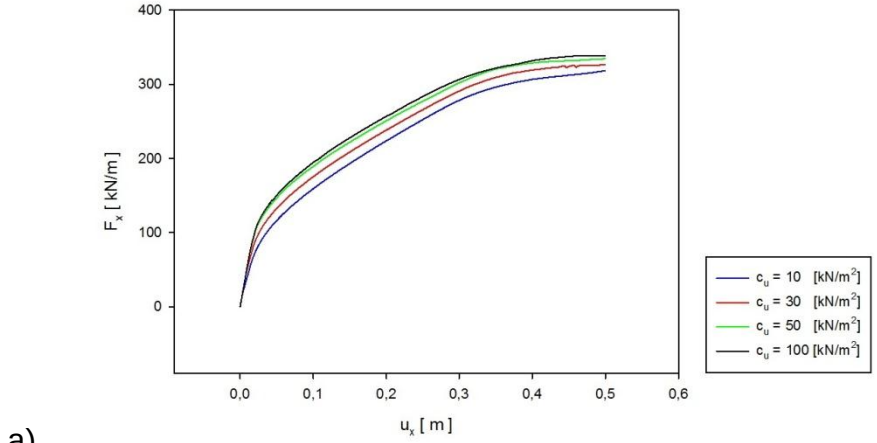

a)

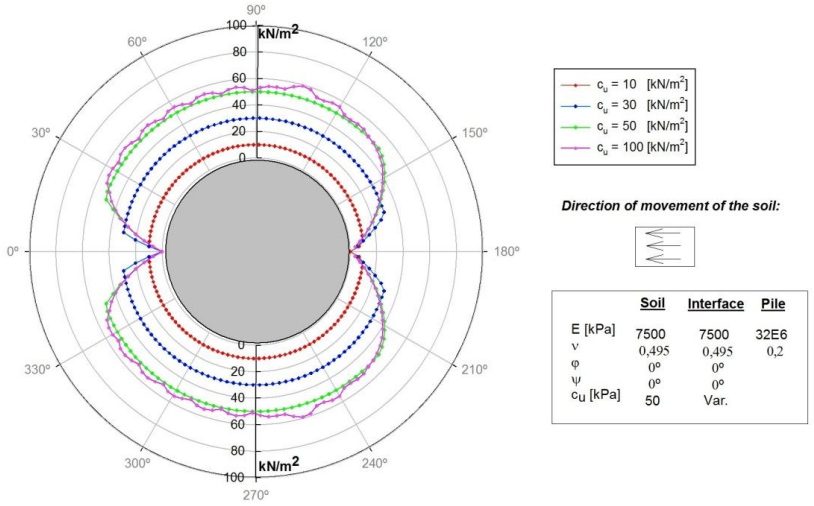

b)

Fig. 4.38 - Lateral forces on half pile versus displacement for variation of c_u in the interface and Shear stress diagram for variation of c_u in the interface

4.8.2 Variation of E_u in the interface properties

Fig. 4.39 shows the influence of the undrained Young's modulus on the normal stress diagram for a displacement of 2 cm. With the increase of the undrained Young's modulus it is registered also a small increase of the normal stress. As well as for the variation of the undrained cohesion in the interface, this increase is registed until the Coulomb criterion is applyed, what happens for a undrained Young's modulus of 5000 and 10000 kN/m^2.

The influence of the undrained Young's modulus on the reaction force of the pile is shown in Fig. 4.40.a), which shows the force - displacement curves for half pile. It can be seen that with the increases of the undrained Young's modulus the ultimate force pratically does not change.

Fig. 4.40.b) shows the influence of undrained Young's modulus on the shear stress diagram for a displacements of 2 cm. It can be seen that with the increases of undrained Young's modulus, also the value of the shear stress increase until reaching the value of the undrained cohesion (50 kN/m^2) and the Coulomb criterion been applied.

Tab. 5 shows the influence of the undrained Young's modulus on the displacement of the soil. The values of displacements are calculated for the same point that were calculated for the study of the c_u (Point 4.8.1). It can be seen that with the increase of E_u the displacements decrease.

It is possible to conclude that the interface parameters (E_u and c_u) has a low influence in the ultimate force applied on the pile and on the normal stress diagram. However, the interface parameters has a relevant influence on the displacements of the soil around the pile and in the shear stress diagram which control the transition from the elastic behavior to the plastic behavior in the interface. However, the undrained Young's Modulus has influence on the shear stress diagram but not on the maximum value.

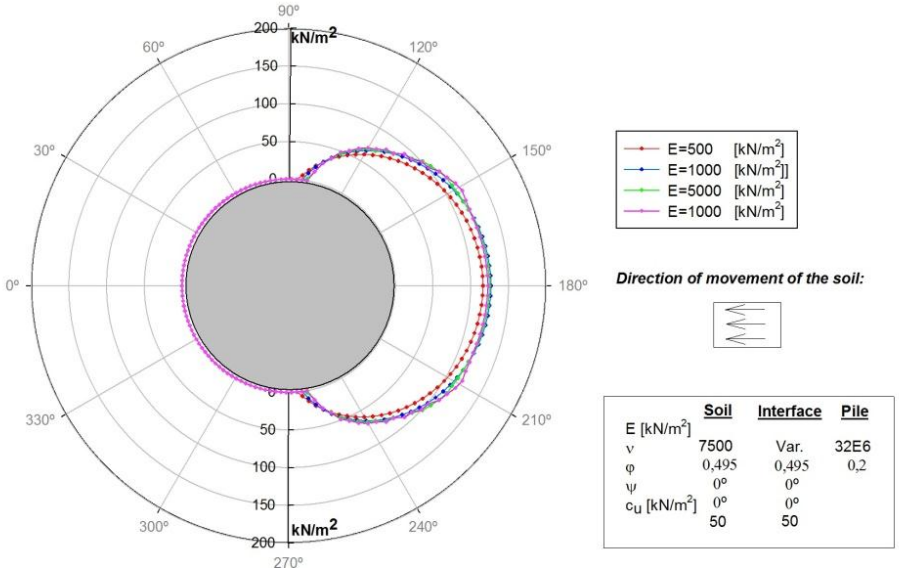

Fig. 4.39 - Normal stress diagram for variation of E_u in the interface

E_u kN/m^2	Displacement m
500	0,014
1000	0,012
5000	0,0105
10000	0,0103

Tab. 5 - Displacements for variation of E_u (point 0º)

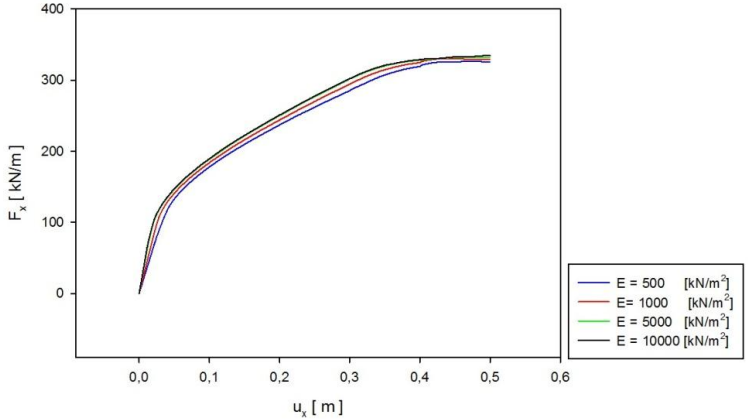

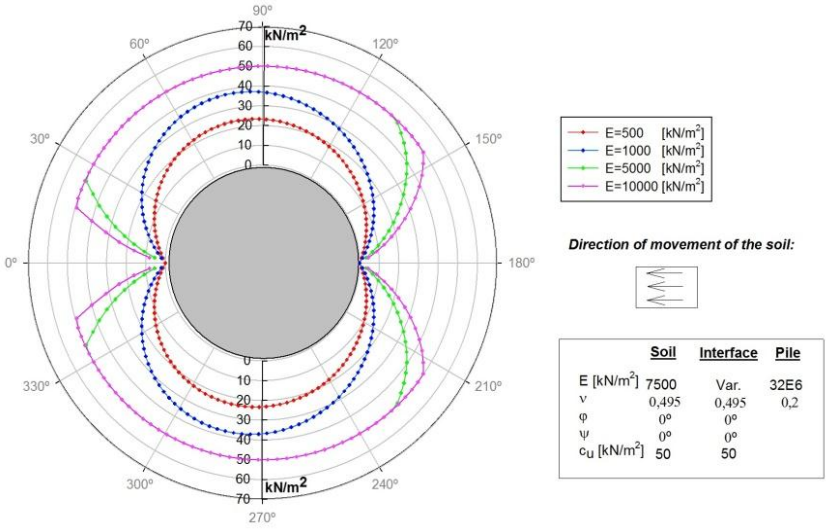

Fig. 4.40 - Lateral forces on pile versus displacement for variation of E_u in the interface properties and shear stress diagram for variation of E_u in the interface

4.8.3 Variation of c_u in the soil properties

To performe the calculations presented in this point were used the same parameters for the interface and for the soil, in order to simulate a total rougness between the soil and pile, making it impossible to study the effect of the variation of the undrained cohesion in the soil parameters.

In Fig. 4.41 is presented the influence of the undrained cohesion on the normal stress diagram for a displacement of 2 cm. With the increase of the undrained cohesion the normal stress also increase. However, for 2 cm the load-displacement is in the very begining and the difference on the normal stress diagram is not relevent. With the increase of the displacements, this difference will increase until reach a maximum when the ultimate force is archived

Fig. 4.42.a) shows the influence of the undrained cohesion on the reaction force in half pile. It can be seen that with the increase of the undrained cohesion is recorded a significant variation of the ultimate force. Due to the fact of the plot show the lateral force in half pile the value of the ultimate force is always around $6{,}25c_u$. For a intire pile this value has to be multiplied by 2 and the value obtained is $12{,}5c_u$ what is in agreedment with the values presented in this research study. The linearity is approximately the same for small displacements. With the incease of the undrained cohesion, the rate of increases of lateral force on the pile for intermediate displacements also increases.

Fig. 4.42.b). This figure shows the influence of changing undrained cohesion in the interface properties. However, the change of interface parameters for differents calculations are necessary in order to provide the total "roughness" between pile and soil and is shown in point 4.8.1 that the shear stress diagram it is controled by the properties in the interface (undrained cohesion).

Tab. 6 shows the influence of the undrained cohesion on the displacement of the soil. The values of displacement were calculated for the same point that was

calculated for the study of c_u in the interface properties in Point 4.8.1. It can be seen that with the increase of c_u the displacements decrease.

As conclusion, the change of the cohesion in the soil parameters has a major influence on the ultimate force and on the normal stress diagram. The value of ultimate force is approximately $12,5c_u$ for the entire pile and the soil has an increase of displacement around the pile.

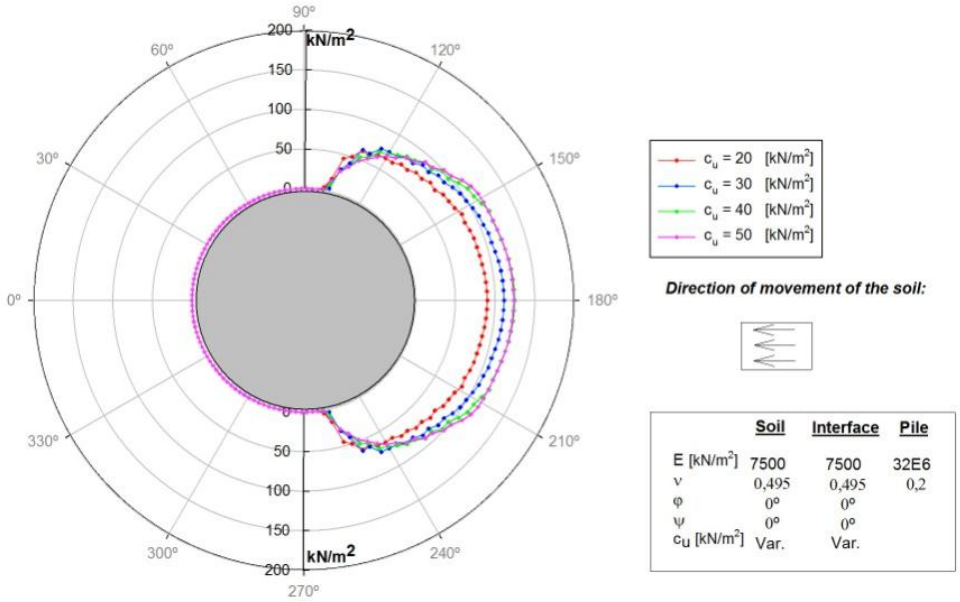

Fig. 4.41 - Normal stress diagram for variation of c_u in the soil for a displacement of 2 cm

c_u kN/m^2	Displacement m
20	0,014
30	0,013
40	0,012
50	0,010

Tab. 6 - Displacements for variation of cu in the soil parameters (point 0º)

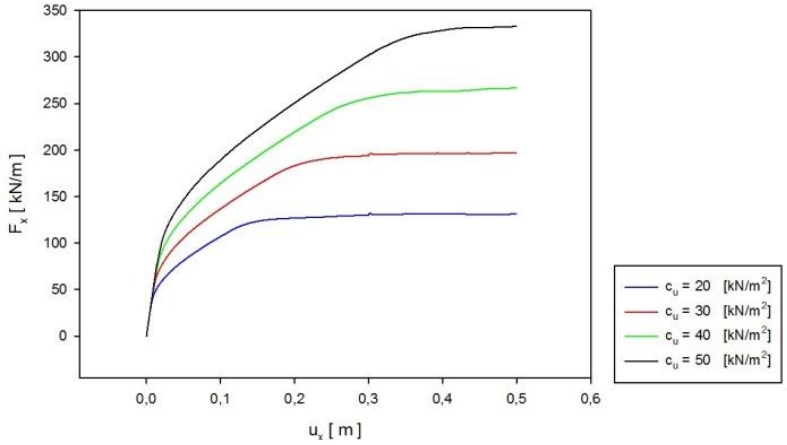

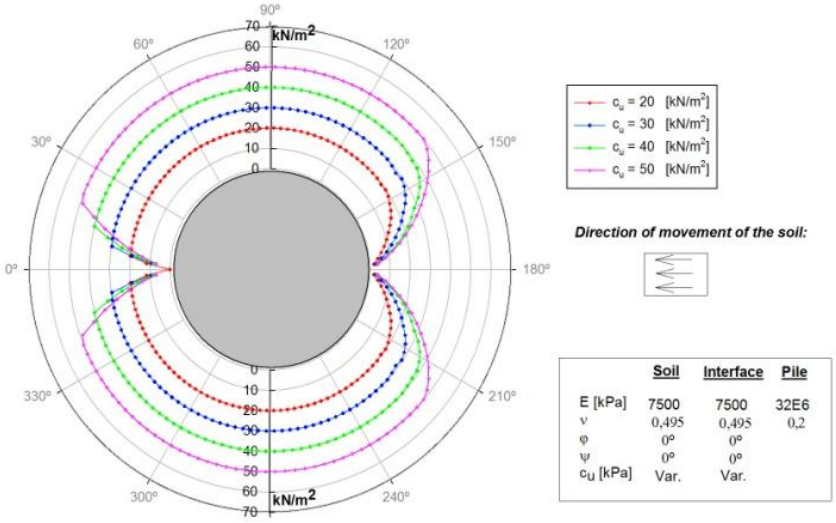

Fig. 4.42 - Lateral forces on pile versus displacement for variation of c_u in the interface properties and shear stress diagram for variation of c_u in the interface

4.8.4 Variation of E_u in the soil properties

Fig. 4.44 shows the undrained Young's modulus influence on the normal stress diagram for a displacement of 2 cm. As expected for small displacements, the increase of the undrained Young's modulus also increases the normal stress in the back of the pile. For intermediate displacements is expect that this diference increase and for large displacements, when the ultimate force is archived, the normal stress diagram will be the same independetly of the Young's modulos.

The influence of undrained Young's modulus on the reaction force on half pile it is shown in Fig. 4.45.a). The ultimate force remains the same for diferent values of E_u, since that is controled by the undrained cohesion, as seen at point 4.8.3. However, it is observed an increase of horizontal force at the pile with the increase of the undrained Young's modulus for intermediate displacements.For lower values of E_u is needed more displacement to reach the ultimate force.

Fig. 4.45.b) shows the undrained Young's modulus influence on the shear stress diagram. As seen at point 4.8.1, the shear stress diagram is controled by the c_u in the interface properties, which means that the undrained Young's modulus has no influence on this results.

Tab. 7 shows the undrained Young's modulus influence on the displacement of the soil. The values of displacement were calculated from the point where the biggest gap displacement happens, which in this case is in the back of the pile (0^o). It can be seen that with the increase of the undrained Young's modulus the value of the displacement also increase.

The undrained Young's modulus has a higher influence on the normal stress diagram and on the reaction force for small and intermediates values of displacement, in the dispacement needed to reach the ultimate force and on the displacement of the soil around the pile.

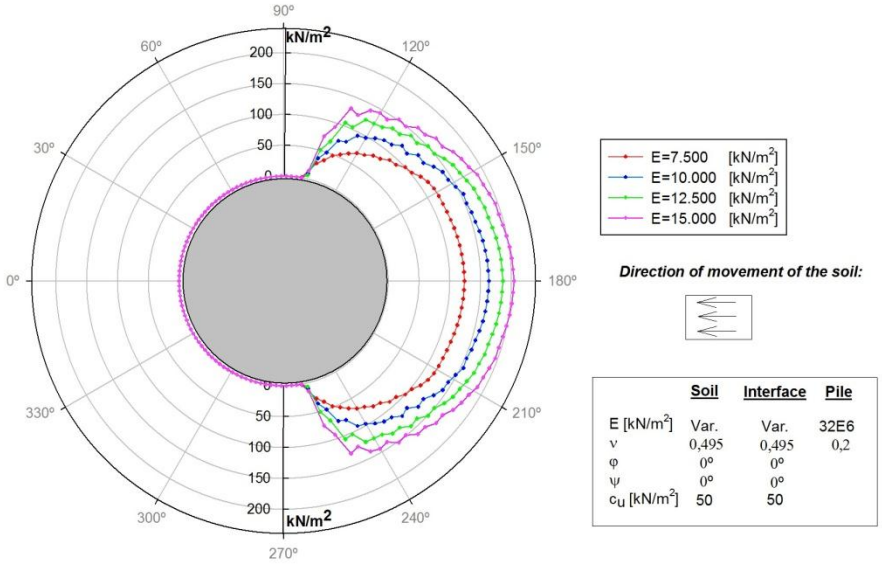

Fig. 4.44 - Normal stress diagram for variation of E_u in the soil for a displacement of 2 cm

E_u kN/m^2	Displacement m
7.500	0,010
10.000	0,012
12.500	0,013
15.000	0,014

Tab. 7 - Displacements for variation of E_u in the soil properties (point 0º)

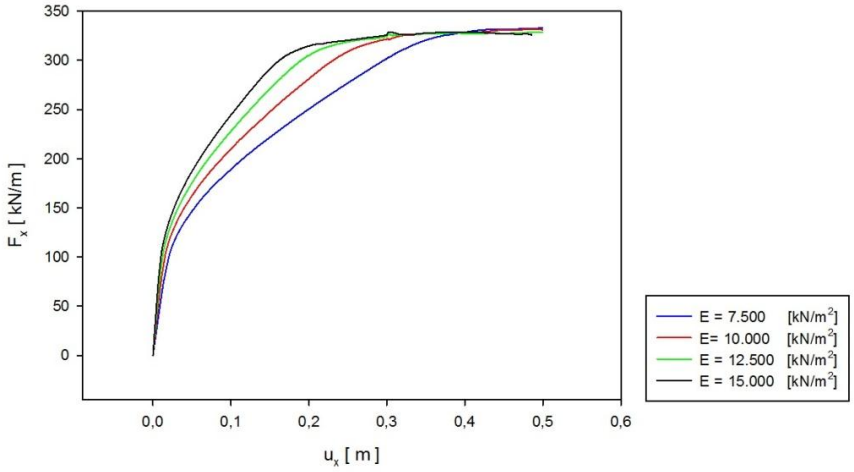

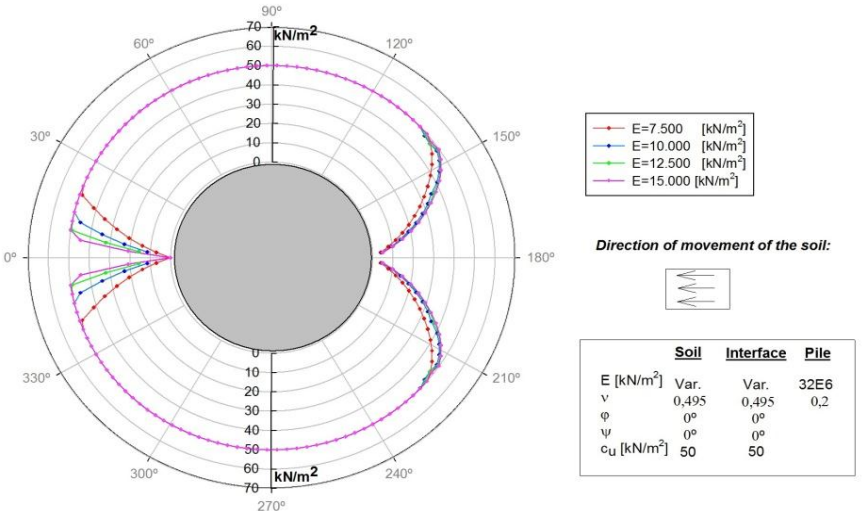

Fig. 4.45 - Lateral forces on half pile versus displacement for variation of E_u in the soil properties and Shear stress diagram for variation of E_u in the soil

4.8.5 Influence of the virtual thickness factor

To carried out these calculation, the properties from the soil and interface remain unchanged only changing the value of the virtual thickness factor (V.T.F.). The interface undrained cohesion was set to 100 kN/m^2 in order to prevent any influence of Coulomb criterion on the results.

Fig. 4.46 and Fig. 4.47.a shows the influence of the virtual thickness on the normal stress diagram and on the total force applied at half pile. It can be seen that the virtual thickness has no influence in both.

Fig. 4.47.b) shows the shear stress diagram for the variation of the virtual thickness. It can be seen that with the increase of the virtual thickness factor the value of the shear stress has a relevant decrease. Excepting the shear stress for V.T.F.=0,1, it can be seen that the shear stress decrease linearly with the increase of the value of t_i. This results are in agreedment with the theory presented in point 3.2.5.1 where the formulation envolving this parameter is explained taking into account the study developed and the information given by the manual of PLAXIS. However, the diference from the shear stress for V.T.F.=0,1 to 0,3 is almost zero and if the value of the V.T.F. decrease under 0,1 this diference will not change. This prove that something is missing in the formulation presented in point 3.2.5.1 where the interface element formulation is explained. Without access to a more detailed formulation for the interface elements, this behavior is not possible to be explained.

Tab. 8 shows the displacements for the variation of the virtual thickness (point 0º). It can be seen that there is a relevant increase of the displacements with the increase of the virtual thickness.

It can be concluded that with the increase if the virtual thickness the displacements increase and the shear stress decrease, as expected.

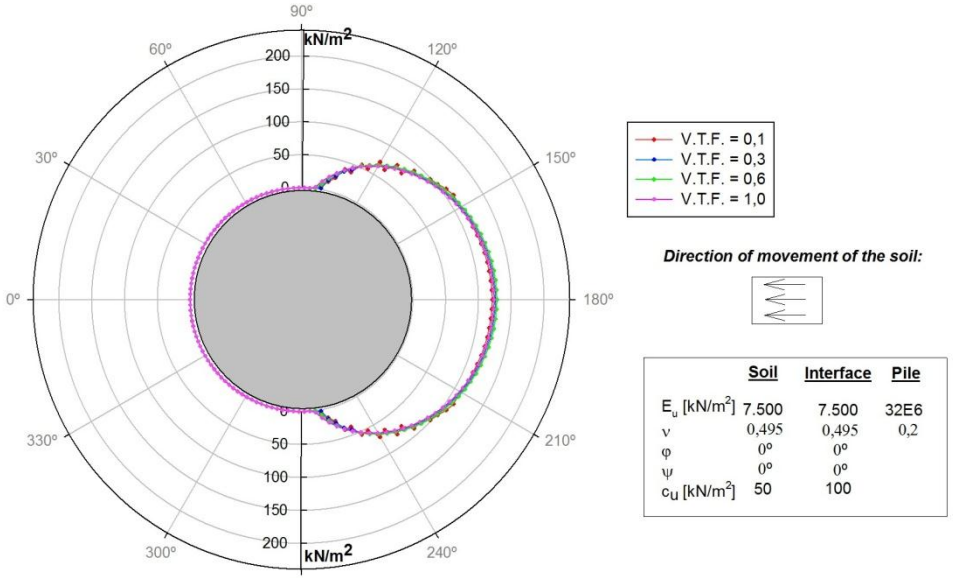

Fig. 4.46 - Normal stress diagram for variation of virtual thickness factor

V.T.F.	Displacement m
0,1	0,010
0,3	0,011
0,6	0,012
1,0	0,014

Tab. 8 - Displacements for variation of virtual thickness factor (point 0º)

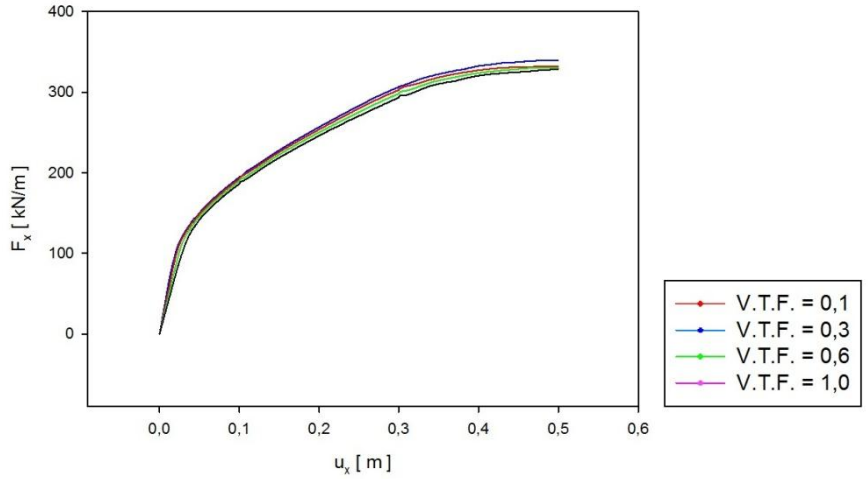

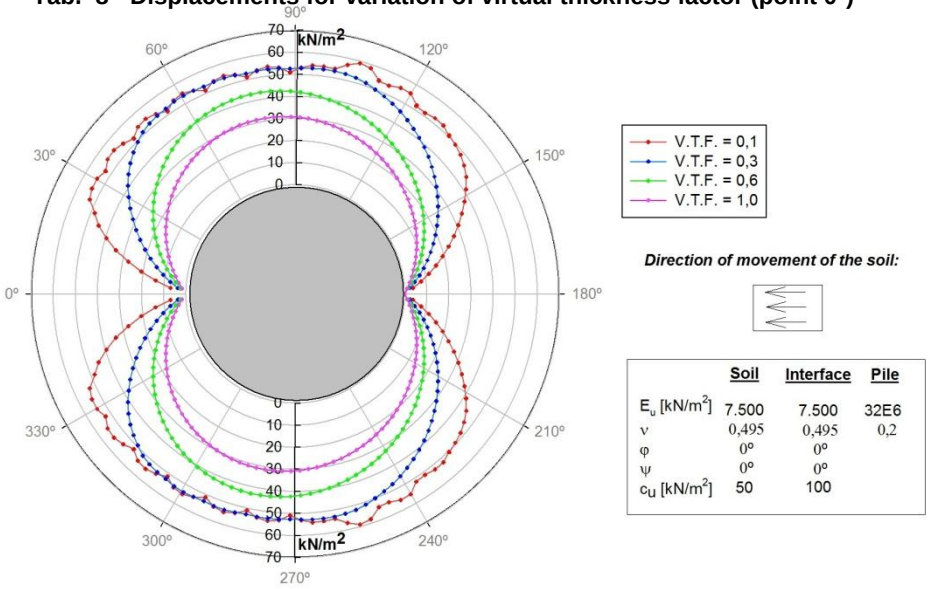

Fig. 4.47 - Lateral force on half pile versus displacement for variation of virtual thickness factor and Shear stress diagram for variation of virtual thickness factor

4.8.6 Influence of the pile diameter

In this point is presented the influence of the pile diameter in the horizontal total force applied on the complete pile.

Fig. 4.48 shows the horizontal total force applied on the pile for a value of undrained cohesion of 10 kN/m^2 and for different pile diameters. It can be seen that the pile diameter has direct influence on the total force applied on the pile, increasing the total force with the increase of the pile diameter. The total force increase linearly with the increase of the pile diameter, what means that the pressure applied on the pile does not change.

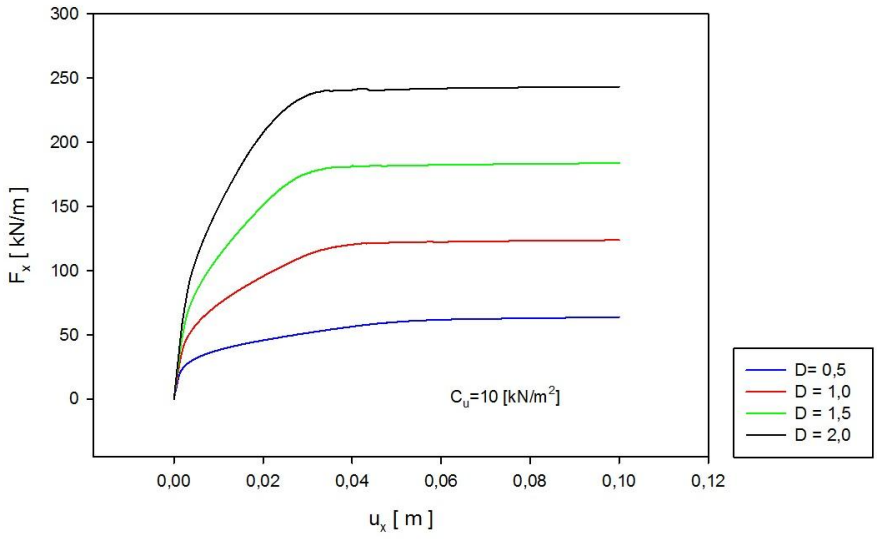

Fig. 4.48 - Horizontal total force applied on the complete pile for a undrained cohesion of 10 kN/m^2 without initial stress (depth= 0 m)

It is possible to conclude that the calculation of the ultimate force applied on the pile due to horizontal movements of the soil (clays) can be easily calculated using the following formula:

$$F_{x,ult} = P_{x,ult} * D_{pile} \qquad \text{Eq. 28}$$

with $F_{x,ult}$ the horizontal ultimate force applied on the pile, $P_{x,ult}$ the ultimate soil pressure applied on the pile and D_{pile} the pile diameter. The value of ultimate

soil pressure $P_{x,ult}$ resulting from the current study is 12,7c_u, as show in Chapter 4.5.1 - Influence of Depth.

4.9 Conclusion

The problem analyzed on this research study fits into a large deformation problem. From the analyze to the results obtained, it was found that the modeling of the pile subjected to a passive load were not the most appropriate. In reality, PLAXIS is more appropriate to the modeling of small deformations, what covers the majority of the geotechnical problems.

5 FURTHER STUDIES

In this chapter are presented some studies that during this research were considered of interest. The topics covered are the overlapping of the mesh, the shear stress diagram when gap occurs, the restoration of pile - soil contact and the Arbitrary Lagrangian-Eulerian method (ALE).

5.1 Overlapping of the mesh

One of the topics studied was the overlapping of the two meshes (the mesh from the soil over the mesh from the pile, Fig. 5.1). After carried out some calculations, it was found that if the Young's modulus increases and decrease the virtual thickness factor of the interface the overlap will decrease. It seems that this behavior occurs because of the interface stiffness, which was explained at point 3.2.5.3. However, it needs to have some more studies to confirm this hypotheses or even if this is other kind of problem.

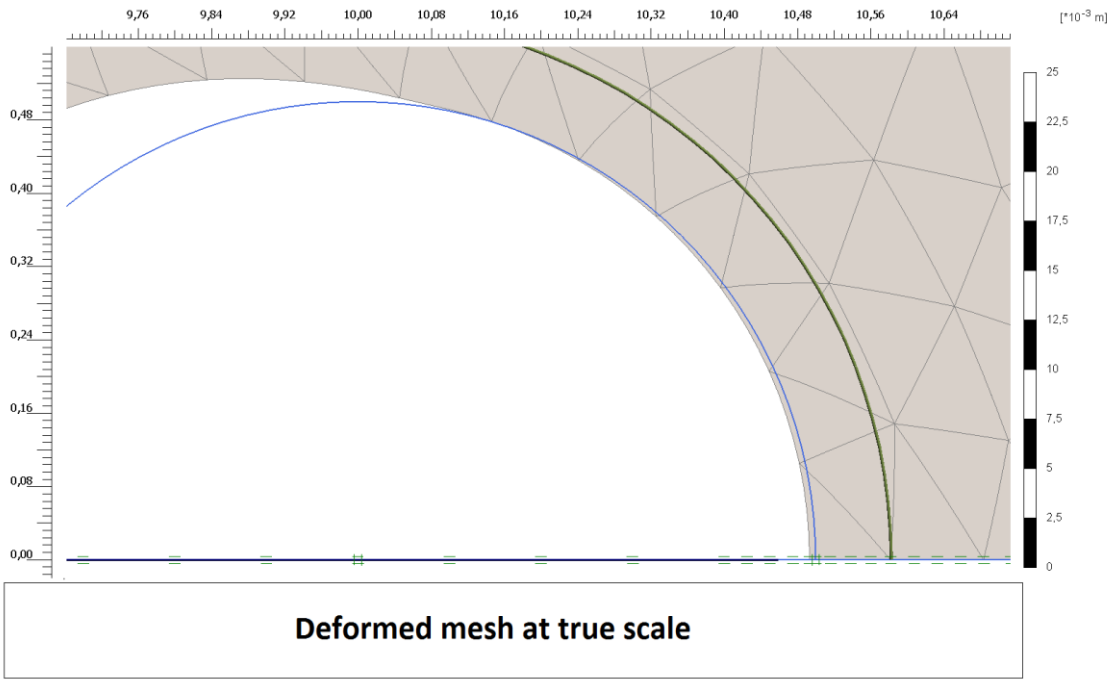

Fig. 5.1 - Overlapping of the mesh from the soil into the mesh from the pile

5.2 Shear stress diagram when gap occurs

The formulation of PLAXIS for the interface allows both gap and slip displacements at the same time. It means that is possible to have gap, with shear stress and normal stress, what is not realistic. Fig. 5.2 shows a representation of how is generated the shear and the normal stresses along the interface. It can be seen that even when gap occurs, elements continue to have deformation, leading to generation of shear and normal stresses.

The solution for the problem of the normal stress in the zone of gap is the use of the option "tension cut-off", what means that the allowable tensile strength may be entered, and set the tensile strength to zero. The only possibility to have a behavior of shear stress close to what is expectable is to use the Coulomb criterion to control the shear stress, setting the cohesion to zero as shown in point 4.4.3.2 , what leads to a direct influence of the normal stress and the friction angle in the shear stress diagram. The stresses presented by PLAXIS are the stresses in the interface and not in the pile.

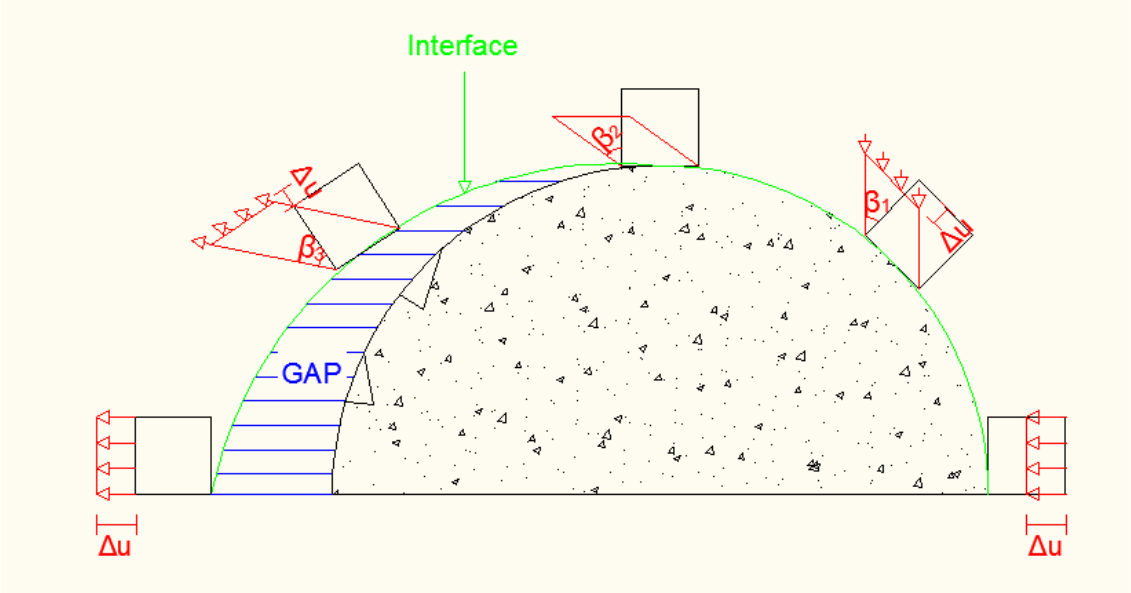

Fig. 5.2 - Representation of the generation of normal and shear stresses in the interface

5.3 Restoration of the pile-soil contact

Another important aspect of the pile soil interface behavior is the restoration, or rebounding of the pile soil contact. Some calculations were developed in order to explore this situation were the same characteristics of the previous calculations were used. First, a displacement is applied in both boundaries, in order to simulate the movement of the soil (u=-0,02[m]). After that, the direction of the displacement is changed in the opposite direction (u=-0,00[m] and u=0,02[m]). Is expected that the contact between pile and soil is being restored again, and normal and shear stresses will gradually be recovered. This behavior was not observed in the calculations developed, the interface did not restored the soil-pile contact.

When the direction of the flow is changed in the opposite direction, the program assumes that the soil in gap is already in contact with the pile and behaves as the restoration is already done (Fig. 5.3). This means that after working in tensile stress changes to compression immediately and vice-versa, i.e. it has no gradual changing.

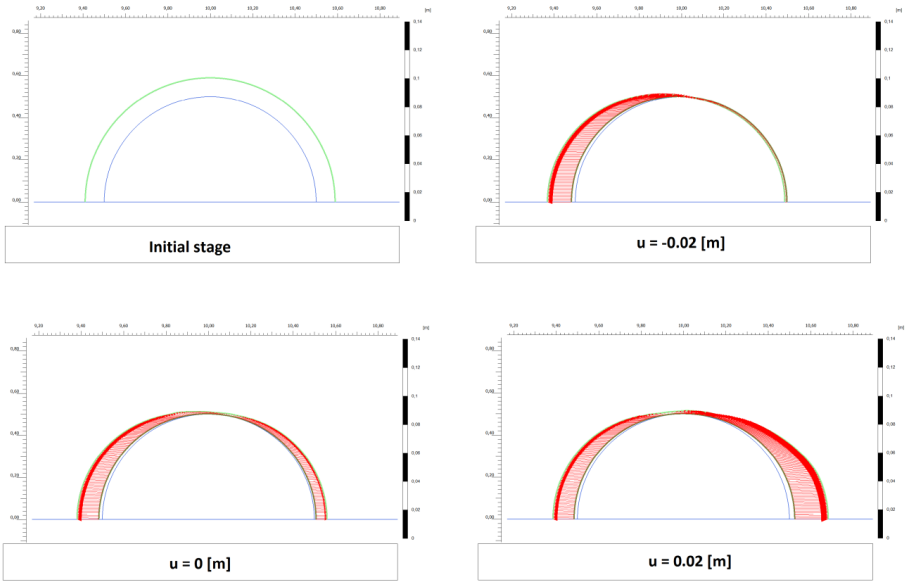

Fig. 5.3 - Magnitude and direction of the displacement of the interface for the case of soil pile contact restoration

5.4 Arbitrary Lagrangian-Eulerian Method

In the study case, the material undergoes very big deformations. These deformations distort the finite element mesh, often to the point were: the mesh is unable to provide accurate results; or the analysis terminates for numerical reasons. Due to the advanced techniques used by the finite element program ABAQUS, as Arbitrary Lagrangian-Eulerian method (ALE), it is believed that this program is a good option for solve big deformation problems. ALE method uses a single mesh definition that is gradually smoothed within analysis steps. The term ALE implies a broad range of analysis approaches, from purely Lagrangian analysis, in which the node motion corresponds to material motion, to purely Eulerian analysis, in which the nodes remain fixed in space and material "flows" through the elements. ALE analysis use an approach between these two extremes: The equilibrium equations are solved on the basis of a deforming mesh with Update Lagrange - Finite Element Method (UL-FEM). However, the displacements of nodes do not necessarily coincide with the movements of particles of the solid body throughout a computation. If mesh distortions become too large, nodes might be uncoupled from the particles that they follow. Thus, particles of the solid body (its state or material parameters) move relative to the nodes of the mesh, which correspond to an Eulerian approach.

The contact formulation from ABAQUS differs from the interface formulation from PLAXIS. While in PLAXIS the contact between two materials is simulated using interface elements and their properties are assigned by the user, in ABAQUS several contact formulations are available and each formulation is based on a choice of a contact discretization, a tracking approach, and assignment of "master" and "slave" roles to the contact surfaces. ABAQUS-Standard offers two contact discretization options: a "node-to-surface" discretization and a "surface-to-surface" discretization. With a node-to-surface discretization the contact conditions are established such that each slave node on one side of a contact interface effectively interacts with a point of projection on the master surface on the opposite side of the contact interface (Fig. 5.4).

The slave nodes are constrained not to penetrate into the master surfaces, however, the nodes of the master surface are allow to penetrate into the slave surface.

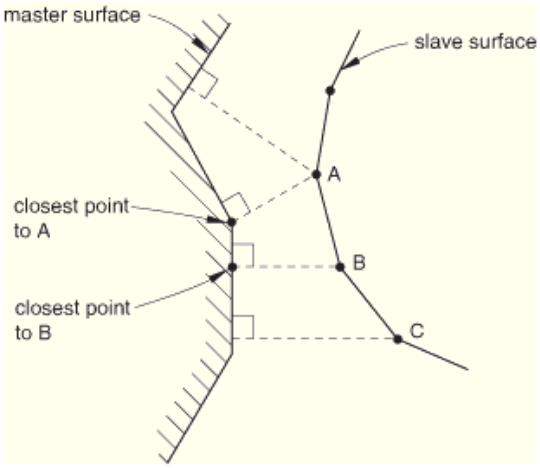

Fig. 5.4 - Node-to-node discretization (ABAQUS documentation V6.8)

In a surface-to-surface contact discretization, the shape of both the slave and the master surfaces are considered in the region of contact. With this discretization, some penetration from master nodes into the slave surface may occur, however, large penetration of master nodes into slave surfaces do not occur with this discretization.

During the development of this research study, some calculations with the finite element program ABAQUS were developed. An overview of what was done is shown below. The model used is showed in Fig. 5.5, in where it is applied a displacement to the pile and the boundaries remain unchanged.

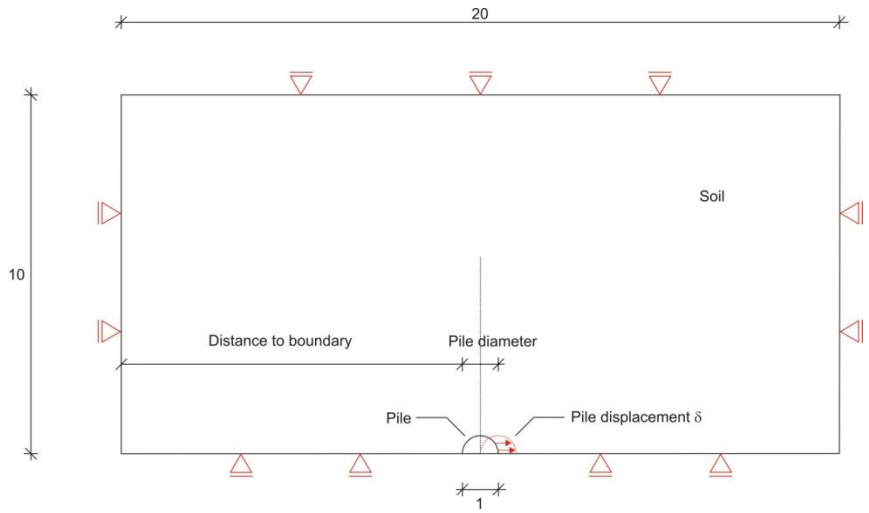

Fig. 5.5 - Model adopted

In Fig. 5.6 is represented the different displacement field for the pile moving and for the soil moving. It can be seen that the soil displacement field obtained with moving the pile is different from the one obtained with moving the soil and is comparable to the deformation mechanism presented by Randolph et al. (1984) (Fig. 5.7).

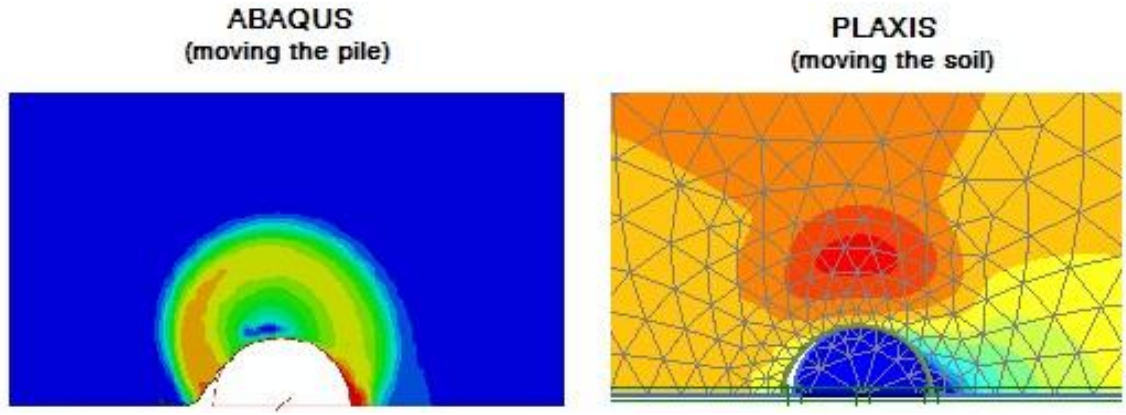

Fig. 5.6 - Displacement field moving the pile using ABAQUS and moving the soil using PLAXIS

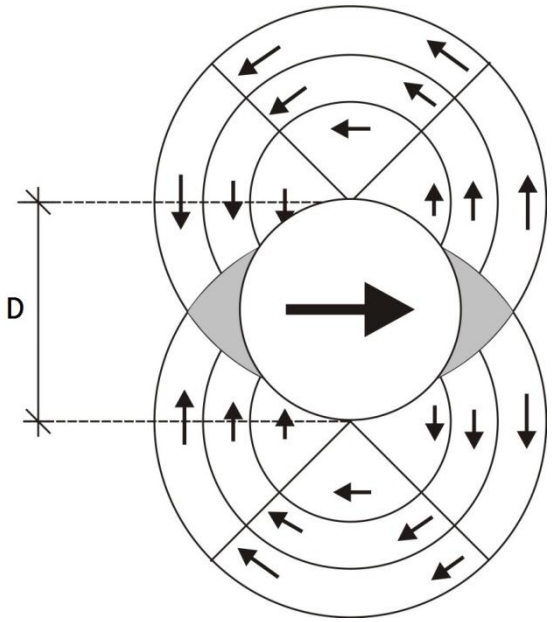

Fig. 5.7 - Deformation mechanism presented in Randolph et al. (1984)

6 CONCLUSIONS

For a conventional small-deformation in a finite element analysis of geotechnical problems, soil-structure interaction is generally well modeled by interface elements and is proved to be a robust and efficient solution. Interface elements model soil-structure interaction by relating relative displacements between pairs of surface nodes of two materials (dual nodes) through constitutive equations for the contact stresses. For large deformations, however, this approach cannot be used in a straightforward manner, as the dual nodes of interface elements has to remain in direct contact. Indeed, interface elements cannot be used with an Update Lagrangian - Finite Element Method (UL-FEM) analysis, as relative displacements between dual nodes, and subsequent remeshing destroy the required contact between dual nodes (Lars Beuth, 2012). For this reason, (master-slave) contact algorithms tend to be applied in UL-FEM formulations (Sheng, 2007).

The shear and normal stresses diagrams presented with the interface elements correspond to what is happening with the interface elements and not what is happening with the contact surface soil/pile, so the interaction soil-structure is not adequate.

In this study, the material undergoes very large deformations. These deformations distort the finite element mesh, often to the point were: the mesh is unable to provide accurate results; or the analysis terminates for numerical reasons.

The normal stress has the main influence on the generation of the lateral force applied on the pile. For a soft cohesive soil in undrained conditions considering a rigid pile, the ultimate pressure applied at the pile obtained with PLAXIS was constante with the variation of depth, depending only from the undrained cohesion. This is due to the fact that it does not take into account the vertical movement of the soil. The value obtained of $12,7c_u$ for the ultimate pressure applied at the pile must be valid only after a certain deep.

Recommendations for future studies

This study case origines many different paths that can be traveled. Some of these paths are set below:

- To extend the research for a row of piles, taking into account the influence of the distance between piles;
- The use of 3-D calculation instead of 2-D, which is more realistic and gives more possibilities to model many complex geotechnical problems, like the interaction soil-structure;
- To consider a advanced constitutive model. Exist many models available, also in PLAXIS, that represent better the soil behavior then the Mohr-Coulomb model.
- To consider more advanced models, as the Arbitrary Eulerian-Lagrangian model (ALE) or the Coupled Eulerian-Lagrangian model (CEL) avaiable in ABAQUS are a promising option.

7 REFERENCES

Adachi, T., Kimura, M., Tada, S. (1989): Analysis on the preventive mechanism of landslide stabilizing piles. Jn: Numerical Models in Geotechnics, Edited by S. Pietruszczak and G.N. Pande, Vol. 111, pp. 691-698.

Alarcon, E., Cano, J.J. (1989): Boundary element approach to the dynamic stiffness functions of circular foundations. Jn: International Journal for Numerical and Analytical Methods in Geomechanics, Vol. 13, pp. 645-664

Almeida, V. S., Paiva, J. B. (2006): Static analysis of soil/pile interaction in layered soil by BEM/BEM coupling. Jn: Advances in Engineering Software, Vol. 38, pp. 835-845.

Bransby, M. F. (1996): Difference between load-transfer relationships for laterally loaded pile grups: active p-y ou passive p-δ. Jn: Geotechnical Engineering, Vol. 122, No. 12, pp. 1015-1018.

Broms, B. (1964): The lateral resistance of piles in cohesive soils. Jn: Soil Mech. Found., ASCE, Vol. 90, oo:27-63.

Brown, D. A.; Reese, L. C.; O'neill, M. W. (1987). Cyclic lateral loading of a large-scale pile group. Journal of Geotechnical and Geoenvironmental Engineering, Vol. 113, No.11, 1326-1343.

Cai, F., Ugai, K. (2011): A subgrade reaction solution for piles to stabilize landslides. Jn: Géotechnique, No. 2, pp. 143-151.

Castelli, F., Maugeri, M. and Motta, E. (1995): Nonlinear analysis of the deflection of a pile subjected to horizontal loads. Revista Italiana di Geotecnia, XXIX, Vol 4, pp. 289-303.

Castelli, F., Maugeri, M. and Motta, E. (1999): Design of Laterally Loaded Piles in Cohesive Soils Using p-y Curves. Jn: Soils and Foundations, Japanese Geotechnical Society. Vol. 39, No. 6, pp. 133-134.

Chaoui, F., Magnan, J. P., Ph. Mestat (1994): Three-dimensional analysis of the behavior of piles in unstable slopes. Jn: Computer Methods and Advances in Geomechanics, pp. 2297-2303.

Chandrasekaran, S.S., Boominathan, A., Dodagoudar, G.R. (2010): Group Interaction Effects on Laterally Loaded Piles in Clay. Journal of Geotechnical and Geoenvirommental Engineering, Vol. 136, ASCE, No. 4, pp. 573-582.

Chen, C.-Y., Martin, G.R. (2002): Soil-structure interaction for landslide stabilizing piles. Jn: Computers and Geotechnics, Vol. 29, pp. 363-386.

Ching, J., Chen, J. (2010): Predicting displacement of augered cast-in-place piles based on load test database. Structural Safety, Vol.32, pp. 372-383.

Davis Waterman, (2006): Structural elements and excavations. Presentation in CG1 Chile.

Escario, V., Uriel, A. (1989): Lateral forces induced on a pier of the "canalejas viaduct" by a slope stabilizing fill.

Finno, R.J., Lawrence, S.A., Allawh, N.F., Harahap, I.S. (1991):Analysis of performance of pile groups adjacent to deep excavation. Jn: Geotechnical Engineering, ASCE, Vol.117, No.6, pp.934-955.

Heyman, L., Boarsma, F. (1961): Bending moments in piles due to lateral earth pressure. Proc. 5th ICSMFE, Paris, Vol.2, pp425-429.

Huang, M., Mu, L. (2011): Vertical response of pile raft foundations subjected to tunneling-induced ground movements in layered soil. International Journal for Numerical and Analytical Methods in Geomechanics. Vol.10, pp. 1002-1035.

Hull, T.S., Lee, C.Y., Poulos, H.G. (1991): Mechanics of pile reinforcement for unstable slope. Research report submitted to National Technical Information Service, U.S. Department of Commerce, Report No. R-636.

Ilyas, T.; Leung, C. F.; Chow, Y. K.; Budi, S. S. (2004). Centrifuge model study of laterally loaded pile groups in clay. Journal of Geotechnical and Geoenvironmental Engineering, Vol.130, No.3, pp: 274-283.

Ito, T., Matsui, T. (1975): Methods to estimate lateral force acting on stabilizing piles. Jn: Soil and Foundations, Vol. 15, pp. 43-59.

Ito, T.; Matsui, T (1977): The effects of piles in a row on the slope stability, proceedings, 9th I.C.S.M.F.E., Special Session. 10, Tokyo.

Ito, T.; Matsui, T (1978): Discussions: Methods to estimate lateral force acting on stabilising piles. Jn: Soils Found, 18(2), pp:41-44.

Ito, T., Matsui, T., Hong WY (1979): Design method for the stability analysis of the slope with landing pier. Jn: Soils Found, 19(4), pp: 43-57.

Jeong, S., Kim, B., Won, J., Lee, J. (2003): Uncoupled analysis of stabilizing piles in weathered slopes. Jn:Computers and Geotechnics, Vol. 30, pp. 671-682.

Janoyan, K.D., Stewart, J. P., Wallace, J. W. (2001): Analysis of p-y Curves from Lateral Load Test of Large Diameter Drilled Shaft in Stiff Clay. Proc. Caltrans 6th Seismic Design Workshop, University of California, Los Angeles.

Kahyaoglu, M. R., G. Imancli, Ozturk, A. U., Kayalar, A.S. (2009): Computational 3D finite analyses of model passive piles. Journal Computational Materials Science, Vol. 46, pp. 193-202.

Kalteziotis, N., Zervogiannis, Frank, R., Seve, G., Berche, J. C. (1993): Experimental study of landslide stabilization by large diameter piles. Jn: Geotechnical Engineering of Hard Soils-Soft Rocks, ISBN, pp.1115-1124.

Karthigeyan, S., Ramakrishna, V. V. G. S. T., Rajagopal, K. (2007): Numerical Investigation of the Effect of Vertical Load on the Lateral Response of Piles. Journal of Geotechnical and Geoenvironmental Engineering, ASCE, Vol. 124, No. 7, pp.846–856.

Katzenbach, R., Pokpong, S. (2007): Numerical simulation of passively loaded piles adjacent to embankment constructed on soft Bangkok clay. Soft Soil Engineering. Darmstadt University of Technology.

Kim, Y., Jeong, S., Won, J. (2009): Effect of lateral Rigidity of Offshore Piles Using Proposed p-y Curves in Marine Clay. Jn: Marine Georesources and Geotechnology, Vol.27, pp. 53-77.

Kim, Y., Jeong, S. (2010): Analysis of soil resistance on laterally loaded piles based on 3D soil-pile interaction, Jn: Computers and Geotechnics, No. 38, pp. 248-257.

Koiter, W. T. (1960): General theorems for elastic-plastic solids. Jn: Progress in Solid Mechanics, North-Holland, Amsterdam, pp. 165-221.

Lars Beuth, 2012: Formulation and Application of a Quasi-Static Material Point Method. PhD thesis, Institut für Geotechnik der Universutät Stuttgart.

Lee, C.Y., Hull, T.S., Poulos, H.G. (1995): Simplified pile-slope stability analysis. Jn: Computers and Geotechnics, Vol. 17, pp. 1-16.

Leung, C.F., Chow, Y.K., Shen, R. F. (2000): Behavior of Pile Subject to Excavation-Induced Soil Movement. Journal of Geotechnical and Geoenvironmental Engineering, ASCE,Vol. 126, No.11, pp. 947-954.

Liang, R.Y., Yamin,M. (2010): Three-dimensional finite element study of arching behavior in slope/drilled shafts system. International Journal for Numerical and Analytical Methods in Geomechanics, Vol. 34, pp. 1157-1168.

Liang, R. Y., Zeng, S. (2002):Numerical study of soil arching mechanism in drilled Shafts for slope stabilization. Soil and Foundations, Japanese Geotechnical Society, Vol. 42, No. 2, pp. 83-92.

Lin, S., Liao, J., Chen, J.T., Chen, L. (2005): Lateral performance of piles evaluated via inclinometer. Jn: Computers and Geotechnics, Vol. 32, pp. 411-421.

Liyanapathirana, D.S., Poulos, H.G. (2010): Analysis of pile behavior in liquefying sloping ground. Journal of Computers and Geotechnics, Vol. 37, pp. 115-124.

Loehr, J.E., E.C. Ang, J.R.. Parra, Bowders, J.J (2004): Design methodology for stabilizing slopes using recycled plastic reinforcement. Jn: Geotechnical Engineering for Transportation Projects, M.K. Yegian and E. Kavazanjian, Editors, ASCE, GSP 126, Vol. 1, pp.723-731.

Loganathan N, Poulos, HG. (1998): Analytical prediction for Tunnelling-induced ground movement in clays. Journal of Geotechnical and Geoenvironmental Engineering. ASCE. 124(7):846–856.

Matos Filho, R., Mendonça, A.V., Paive, J.B. (2005): Static boundary element analysis of piles submitted to horizontal and vertical loads. Jn: Engineering and Analysis with Boundary Elements, Vol. 29, pp. 195-203.

Matlock H. (1970): Correlations for design of laterally loaded piles in soft clay. Proceedings of the 2th annual offshore technology conference, Vol. 1. Houston, TX, Paper ITC 1204, pp. 577-594.

Matsui, T., Hong, W.P. and Ito, T. (1982): Earth pressures on piles in a row due to lateral soil movements. Jn: Soils and Foundations. 22 ("), pp:71-81.

Mendonça, A.V., de Paiva, J. B. (2000): A noundary element method for the static analysis of raft foundations on piles. Jn: Engineering and Analysis with Boundary Elements, Vol. 24, pp. 237-247.

Miao, L.F., Goh, A.T.C., Wong, K. S., Teh, C. I., (2005): Three-dimensional finite element analyses of passive pile behavior. International Journal for Numerical and Analytical Methods in Geomechanics, Vol. 30, pp. 599-613.

Millán, M.A., Domínguez, J. (2009): Simplified BEM/FEM model for dynamic analysis of structures on piles and piles groups in viscoelastic and poroelastic soils. Jn: Engineering Analysis with Boundary Elements, Vol . 33, pp. 25-34.

Ong, D.E.L., Leung, C. F., Chow, Y. K. (2009):Behavior of Pile Groups Subject to Excavation-Induced Soil Movement in Very Soft Clay. Journal of Geotechnical and Geoenvironmental Engineering, ASCE, Vol. 135, No. 10, pp. 1462-1474.

Padrón, L.A., Aznárez, J.J., Maeso, O. (2007): BEM-FEM coupling model for the dynamic analysis of piles and pile groups. Jn: Engineering Analysis with Boundary elements, Vol. 31, pp. 473-484.

Padrón, L.A., Aznárez, J.J., Maeso, O. (2011): 3-D boundary element-finite method for the dynamic analysis of piled buildings. Jn: Engineering Analysis with Boundary elements, Vol. 35, pp. 465-477.

Pan, J. L.; Goh, A. T. C.; Wong, K. S.; Selby A. R. (2002): Three-dimensional analysis of single pile response to lateral soil movements. International Journal for Numerical and Analytical Methods in Geomechanics, Vol. 32, pp. 747-758.

Poulos, H.G. (1973): Analysis of piles in soil undergoing lateral movements. Journal of the Soil Mechanics and Foundations Divisions, Vol. 99, pp:391-406.

Poulos, H. G.; Davis, E. H. (1980). Pile foundation analysis and design. Wiley, New York.

Poulos, H. G.; Chen, L.T., Hull, T.S. (1995): Model tests on single piles subjected to lateral soil movement. Jn: Soils and Foundation, Vol. 35, No.4, pp: 85-92.

Randolph, M.F. (1981): Pilot study of lateral loading of piles due to soil movement caused by embankment loading. Report for the Department of Transport, Engineering Department, Cambridge University.

Randolph, M. F., Houlsby, G. T. (1984): The limiting pressure on a circular pile loaded laterally in cohesive soil. Jn: Géotechnique, Vol. 34, No. 4, pp: 613-623.

Randolph, M.F., Springman, S.M. (1991): Analysis of pile response due to external loads and soil movement. Proc. 10th European Conference on Soil Mechanics and Foundation Engineering, Firenze, Vol.2, pp. 525-528.

Rollins, K. M.; Peterson, K. T.; Weaver, T. J. (1998). Lateral load behavior of full-scale pile group in clay. Journal of Geotechnical and Geoenvironmental Engineering, Vol.124, No.6, pp: 468-478.

Rowe, R.K., Poulos, H.G. (1979): A method for predicting the effect of piles on slope behavior. Proc. 3rd International Conference on Numerical Methods in Geomechanics, Aachen, pp. 1073-1085.

Sheng, D., (2007): Finite element modeling of penetration problems in geomechanics. In proceedings of the 10th international symposium on numerical models in geomechanics, Vol. 10, pp 239-245. Taylor and Francis Group.

Sheng, D., (2011): Review of fundamental principles in modeling unsaturated soil behavior. Jn: Computers and Geotechnics, Vol. 38, pp. 757-776.

Stein, L. R.; Gentry, R. A.; Hirt, C. W. (1977). Computational simulation of transient blast loading on three-dimensional structures. Jn: Comput Metho Appl Mech, Vol. 11, pp: 57-74.

Stewart, D.P., Jewell, R.J., Randolph, M.F. (1992):Piled bridge abutments on soft clay-experimental data and simple design methods. Proc. 6th Aust.-N.Z. Conf. Geomech., Christhurch, Vol. 1, pp. 199-204.

Stewart, D.P. (1999): Reduction of undrained lateral pile capacity in clay due to an adjacent slope. Jn: Australian Geomech., 34(4), 17-23.

Susuki, H. (1988): The lateral flow of soil caused by banking on soft clay ground. Jn: Soils and Foundations, Vol.28, No. 4, pp. 1-18.

Terzaghi, K. (1955): Evaluation of coefficient of sub grade reaction. Jn: Geotechnique, 5 (4), pp. 297-326.

Van Langen, H., Vermeer, P.A. (1991): Interface elements for singular plasticity points. International Journal for Numerical and Analytical Methods in Geomechanicals, Vol. 15, pp. 301-315.

Viggiani, C. (1981): Ultimate lateral load on piles used to stabilize landslides. In proceedings of X^{th} ICSMFE, Stockholm, Vol. 3, pp: 555-560.

Yang, Z., Jeremic, B. (2005): Study of soil layering effects on lateral loading behavior of piles. Journal of Geotechnical and Geoenvironmental Engineering, Vol 131, ASCE, No.6, pp. 762-770.

Zhang, L. (2009): Nonlinear of laterally loaded rigid piles in cohesionless soil. Jn: Computers and Geotechnics. Vol. 36, pp. 718-724.

Zhang, L., MO Hai-hong, Zhu Zhen-de (2012): Theoretical Elasto-Plastic Solution for Piles Subject to Lateral Soil Movement. 2012 International Conference on Structural Computation and Geotechnical Mechanics, Procedia Earth and Planetary Sceince, Vol. 5, pp. 58-63.

Zhang, R., J. Zheng, H. P., Zhang, L. (2011):Analysis of excavation-induced responses of loaded pile foundations considering unloading effect. Tunneling and Underground Space Technology. Vol. 26, pp. 320-335.

Zhang, C., J.Yu, Huang, M. (2012):Effects of tunnelling on existing pipelines is layered soils. Journal Computers and Geotechnics, Vol. 43, pp. 12-25.